# TITLE: Characterisation of a novel role for the dynamin mechanoenzymes in the regulation of human sperm acrosomal exocytosis

**AUTHORS:** Wei Zhou[1], Amanda L. Anderson[1], Adrian P. Turner[2], Geoffry N. De Iuliis[1], A. McCluskey[3], Eileen A. McLaughlin[1,2] Brett Nixon[1]*

**AFFILIATIONS:** [1]Priority Research Centre for Reproductive Science, School of Environmental and Life Sciences, Discipline of Biological Sciences, University of Newcastle, University Drive, Callaghan, NSW 2308, Australia.

[2]School of Biological Sciences, University of Auckland, Auckland 1142, New Zealand

[3]School of Environmental and Life Sciences, Discipline of Chemistry**,** The University of Newcastle, University Drive, Callaghan, NSW 2308, Australia.

***CORRESPONDING AUTHOR:** Brett Nixon, Priority Research Centre for Reproductive Science, School of Environmental and Life Sciences, Discipline of Biological Sciences, University of Newcastle, University Drive, Callaghan, NSW 2308, Australia.

Ph: + 61 2 4921 6977

Fax: + 61 2 4921 6308

Email: Brett.Nixon@newcastle.edu.au

**RUNNING TITLE:** Dynamin regulates human sperm acrosomal exocytosis

## ABSTRACT

**Study question:** Does dynamin regulate human sperm acrosomal exocytosis?

**Summary answer:** Our studies of dynamin localisation and function have implicated this family of mechanoenzymes in the regulation of progesterone-induced acrosomal exocytosis in human spermatozoa.

**What is known already:** Completion of an acrosome reaction is a prerequisite for successful fertilisation in all studied mammalian species. It follows that failure to complete this unique exocytotic event represents a common aetiology in the defective spermatozoa of male infertility patients that have failed in-vitro fertilization in a clinical setting. Recent studies have implicated the dynamin family of mechanoenzymes as important regulators of the acrosome reaction in murine spermatozoa. The biological basis of this activity appears to rest with the ability of dynamin to polymerise around newly formed membrane vesicles and subsequently regulate the rate of fusion pore expansion. To date however, the dynamin family of GTPases have not been studied in the spermatozoa of non-rodent species. Here we have sought to examine the presence and functional significance of dynamin in human spermatozoa.

**Study design, size, duration:** Dynamin expression was characterised in the testis and spermatozoa of several healthy normozoospermic individuals. In addition, we assessed the influence of selective dynamin inhibition on the competence of human spermatozoa to undergo a progesterone-induced acrosome reaction. A minimum of five biological and technical replicates were performed to investigate both inter- and intra-donor variability in dynamin expression and establish statistical significance in terms of the impact of dynamin inhibition.

**Participants/materials, setting, methods:** The expression and localisation of dynamin in the human testis, epididymis and mature spermatozoa were determined through the application of immunofluorescence, immunoblotting and/or electron microscopy. Human semen samples were fractionated via density gradient centrifugation and the resultant populations of good and poor

quality spermatozoa were induced to capacitate and acrosome react in the presence or absence of selective dynamin inhibitors. The acrosome integrity of live spermatozoa was subsequently assessed via the use of fluorescently conjugated *Arachas hypogea* lectin (PNA). The influence of dynamin phosphorylation and the regulatory kinase(s) responsible for this modification in human spermatozoa were also assessed via the use of in-situ proximity ligation assays and pharmacological inhibition. In all experiments, ≥100 spermatozoa were assessed / treatment group and all graphical data are presented as the mean values ± SEM, with statistical significance being determined by ANOVA.

**Main results and the role of chance:** Dynamin 1 (DNM1) and DNM2, but not DNM3, were specifically localised to the acrosomal region of the head of human spermatozoa, an ideal position from which to regulate acrosomal exocytosis. In keeping with this notion, pharmacological inhibition of DNM1 and DNM2 was able to significantly suppress the rates of acrosomal exocytosis stimulated by progesterone. Furthermore, our comparison of dynamin expression in good and poor quality spermatozoa recovered from the same ejaculate, revealed a significant reduction in the amount of DNM2 in the latter sub-population of cells. In contrast, DNM1 was detected at equivalent levels in both sub-populations of spermatozoa. Such findings are of potential significance given that the poor quality spermatozoa proved refractory to the induction of a progesterone stimulated acrosome reaction. In seeking to identify the regulatory influence of progesterone on DNM2 function, we were able to establish that the protein is a substrate for CDK1-dependent phosphorylation. The functional significance of DNM2 phosphorylation was illustrated by the fact that pharmacological inhibition of CDK1 elicited a concomitant suppression of both DNM2-Ser764 phosphorylation and the overall rates of progesterone induced acrosomal exocytosis.

**Large scale data:** N/A

**Limitations, reasons for caution:** This was an in-vitro study performed mainly on ejaculated human spermatozoa. This experimental paradigm necessarily eliminates the physiological

contributions of the female reproductive tract that would normally support capacitation and acrosomal responsiveness.

**Wider implications of the findings:** This study identifies a novel causative link between dynamin activity and the ability of human spermatozoa to complete a progesterone-induced acrosome reaction. Such findings encourage a more detailed analysis of the contribution of dynamin dysregulation as an underlying aetiology in infertile males whose spermatozoa are unable to penetrate the zona pellucida.

**Study funding/Competing interests:** This research was supported by a National Health and Medical Research Council of Australia Project Grant (APP1103176) awarded to B.N. and E.A.M. The authors report no conflict of interest.

**KEY WORDS:** acrosome reaction, dynamin, human spermatozoa, infertility, sperm maturation

# INTRODUCTION

In all mammalian species that have been studied, completion of an acrosome reaction is accepted as a prerequisite for successful fertilization in vivo (Florman *et al.*, 2004; Avella and Dean, 2011). This unique exocytotic process is initiated by multiple fusion events between the outer acrosomal membrane and the overlying plasma membrane (Barros *et al.*, 1967). As this wave of vesiculation spreads across the anterior region of the sperm head, it facilitates the destabilisation of the acrosomal structure, formation of hybrid membrane vesicles and the concomitant release of acrosomal contents (Barros *et al.*, 1967). This, in turn, enables sperm penetration of the resilient zona pellucida matrix, and provides the cell with access to the oocyte plasma membrane. Recent work has drawn into question the long held view that the acrosome reaction proceeds in an 'all or none' manner, with accumulating evidence suggesting that the process may instead comprise several intermediate phases, each with their own set of functional consequences (Buffone *et al.*, 2012; 2014). Irrespective of this, several features of acrosomal exocytosis, including the relatively slow kinetics at which it proceeds, underscore the highly specialised nature of this secretory process and the prospect that is governed by complex molecular mechanisms (Belmonte *et al.*, 2016).

In keeping with this notion, the capacity to complete a physiological acrosome reaction necessitates that spermatozoa have first completed a process of functional maturation, known as capacitation, during their ascent of the female reproductive tract (Stival *et al.*, 2016). Among the many biochemical and biophysical changes that accompany capacitation, the sperm membrane becomes increasingly fusogenic, owing to alterations in its lipid architecture and the release of decapacitation factors (Nixon *et al.*, 2006; Aitken and Nixon, 2013). These combined events serve to modulate intracellular ion concentrations leading to hyperpolarization of the sperm plasma membrane and triggering complex signalling cascades that culminate in increased protein phosphorylation (Visconti *et al.*, 2011). While these, in turn, prime the cell for completion of an acrosome reaction, the precise physiological stimulus responsible for the induction of this exocytotic event remains a matter of some controversy (Buffone *et al.*, 2014). Indeed, the long held

view that zona pellucida ligands act as the key stimulus for induction of acrosomal exocytosis have recently been drawn into question (Baibakov *et al.*, 2007) in favour of alternative models, which suggest that the timing of the acrosomal exocytosis may actually precede that of zona adhesion (Inoue *et al.*, 2011). Such timing may account for the ability of progesterone, a signalling molecule that sperm encounter within the oviduct prior to zona adhesion, to elicit the induction of acrosomal exocytosis in various species, including the human (Meyers *et al.*, 1995; Meizel *et al.*, 1997; Thérien and Manjunath, 2003). Progesterone, in turn, reportedly acts via its ability to modulate an increase in cytosolic $Ca^{2+}$ levels (Blackmore *et al.*, 1990).

The impetus for further investigation of the regulation of acrosomal exocytosis in human spermatozoa stems, at least in part, from the recognition that a failure to complete this event represents a relatively common aetiology associated with the defective spermatozoa of male infertility patients. Indeed, diagnosis of sperm dysfunction suggests that such a defect may account for almost one third of all cases of failed in-vitro fertilisation in couples seeking recourse to assisted reproductive programs due to male factor infertility (Muller, 2000; Liu and Baker, 2003). Notably, these patients commonly present with otherwise normal semen characteristics, suggesting that the defect may be associated with the molecular machinery responsible for the control of acrosomal exocytosis rather than overt morphological defects in their spermatozoa. While such machinery is undoubtedly complex, our recent work in the mouse model has raised the prospect that the dynamin family of mechanoenzymes may hold a critical role in the regulation of this unique exocytosis event (Reid *et al.*, 2012; 2015).

The dynamin family or proteins comprise a group of large GTPases that have been extensively researched in the context of their ability to manipulate membrane vesicles during the combined processes of endo- and exo-cytosis (Shpetner and Vallee, 1989; Williams and Kim, 2014; Jackson *et al.*, 2015). Such functions are largely attributed to the ability of dynamin to self-oligomerise into cylindrical helices around the neck of nascent vesicles (Antonny *et al.*, 2016). In one of the most widely accepted models of dynamin action, GTP hydrolysis subsequently drives

conformational changes that lead to constriction of both the polymer and the membrane beneath, thus promoting vesicle scission and release from the parent membrane (Morlot and Roux, 2013). It has also been shown that dynamin has the ability to regulate the rate of fusion pore expansion between the membranes and newly formed vesicles, thus controlling the amount of cargo released from the vesicles (Anantharam *et al.*, 2011; Jackson *et al.*, 2015). Such a model is in keeping with the protracted timeframe, and progressive release, of the acrosomal contents that have been documented during acrosomal exocytosis in mammalian spermatozoa (Buffone *et al.*, 2014; Belmonte *et al.*, 2016).

The existence of three canonical dynamin members (DNM1, DNM2 and DNM3), as well as several dynamin–like proteins, has been recorded in mammalian species (Antonny *et al.*, 2016). Being encoded by three different genes, DNM1, DNM2, and DNM3 are characterised by differential patterns of expression within distinct tissues of the body. In this context, DNM1 is predominantly found in the central nervous system (Ferguson *et al.*, 2007), DNM2 is ubiquitously expressed throughout the body (Cook *et al.*, 1994), and DNM3 appears to reside mainly in the brain and testis (Cao *et al.*, 1998). Studies conducted in our own, and independent laboratories, have recently begun to explore the expression and functional significance of dynamin in the male reproductive tract of murine models (Iguchi *et al.*, 2002; Lie *et al.*, 2006; Kusumi *et al.*, 2007; Vaid *et al.*, 2007; Zhao *et al.*, 2007; Reid *et al.*, 2012; 2015; Redgrove *et al.*, 2016; Zhou *et al.*, 2017). Thus, prominent expression of DNM2 has been documented in the mouse testes where the protein appears to localise to developing germ cells (Redgrove *et al.*, 2016). Accordingly, conditional ablation of the *Dnm2* gene leads to the complete arrest of spermatogenesis and a corresponding phenotype of male infertility (Redgrove *et al.*, 2016). DNM1 has been identified in mouse germ cells where it appears to be restricted to the developing acrosome of round spermatids (Reid *et al.*, 2012). However, unlike *Dnm2*, the targeted ablation of *Dnm1* did not precipitate overt changes in germ cell development or male infertility (Redgrove *et al.*, 2016). In contrast, DNM3 expression within the testis appears to have minimal overlap with the germ cell population (Vaid *et al.*, 2007;

Reid *et al.*, 2012). Importantly in the context of this study, we have also shown that both DNM1 and DNM2, but not DNM3, are retained in mature mouse spermatozoa where they co-localise within the peri-acrosomal region of the sperm head (Reid *et al.*, 2012). From this position, DNM1 and DNM2 appear to exert an important regulatory influence over acrosomal exocytosis, such that their selective pharmacological inhibition significantly compromises the ability of mouse spermatozoa to complete a progesterone-induced acrosome reaction (Reid *et al.*, 2012). In agreement with such findings, independent research has shown the DNM2 also forms productive interactions with complexin I (Zhao *et al.*, 2007), an important element of the SNARE family of proteins that themselves have been implicated in regulation of acrosomal exocytosis (Buffone *et al.*, 2014). Accordingly, this interaction has been mapped to the acrosomal region of mouse spermatozoa (Zhao *et al.*, 2007).

Notwithstanding promising data generated thus far in rodent models, to the best of our knowledge, there is presently no research directly exploring the presence and/or functional significance of dynamin isoforms in human spermatozoa. Thus, the aim of this study was to characterise the expression pattern of the canonical dynamin family members (DNM1, DNM2 and DNM3) in the human testis and ejaculated spermatozoa, as well as assess their potential role in the regulation of acrosomal exocytosis in our own species.

## MATERIALS AND METHODS

### Ethics statement

The experiments described in this study were conducted with human semen samples obtained with informed written consent from a panel of healthy normozoospermic donors (University student volunteers) assembled for the Reproductive Science Group at the University of Newcastle. All experiments were performed in accordance with protocols approved by the University of Newcastle Human Research and Ethics Committee.

**Reagents**

Unless specified, chemical regents were purchased from Sigma-Aldrich (St. Louis, MO, USA) and were of molecular biology or research grade. Rabbit polyclonal antibody against dynamin 1 (ab108458) was purchased from Abcam (Cambridge, England, UK); goat polyclonal antibody against dynamin 2 (sc-6400) and IZUMO1 (sc-79543), mouse monoclonal antibody against CDC2 (CDK1) (sc-54) and rabbit polyclonal antibody against CDK5 (sc-173) were from Santa Cruz Biotechnology (Dallas, TX, USA); rabbit polyclonal anti-dynamin 2 (PA5-19800) and sheep polyclonal anti-phospho-dynamin 1 (Ser 778) antibodies were from Thermo Fisher Scientific (Eugene, OR, USA); rabbit polyclonal antibody against dynamin 3 (14737-1-AP) was purchased from Proteintech Group (Chicago, IL, USA); mouse monoclonal antibody against α-tubulin (T5168) was from Sigma-Aldrich. Alexa Fluor 594-conjugated goat anti-rabbit, donkey anti-goat and goat anti-mouse, Alexa Fluor 488-conjugated donkey anti-sheep and goat anti-rabbit were all purchased from Thermo Fisher Scientific. Anti-rabbit IgG-HRP was supplied by Millipore (Chicago, IL, USA) and anti-sheep IgG-HRP was supplied by Abcam. Full details of the primary and secondary antibodies are also provided in Supplemental Table S1. Bovine serum albumin was purchased from Research Organics (Cleveland, OH, USA). D-glucose was supplied by Ajax Finechem (Auburn, NSW, Australia). Percoll, HEPES and nitrocellulose were from GE healthcare (Buckinghamshire, England, UK). Precast 4–20% polyacrylamide gels were purchased from BIO-RAD (Gladesville, NSW, Australia). Minicomplete protease inhibitor cocktail tablets were supplied by Roche (Sandhoferstrasse, Mannheim, Germany). Mowiol 4-88 was from Calbiochem (La Jolla, CA, USA), paraformaldehyde (PFA) was obtained from ProSciTech (Thuringowa, QLD, Australia). Human testis lysate was purchased from Santa Cruz Biotechnology. CDK1 inhibitor (217695) was from Millipore. Dynamin inhibitors, Dynasore and Dyngo 4a were purchased from Tocris Bioscience (Bristol, England, UK) and Abcam, respectively. Dyngo-Ɵ (an inactive chemical analogue of both the Dynasore and Dyngo 4a inhibitors) was generated in our laboratory as previously described (McCluskey *et al.*, 2013).

**Human semen analysis**

All semen samples used in this study were assessed according a specialised methodological checklist (Björndahl *et al.*, 2015). Briefly, semen samples were collected following sexual abstinence of at least two days. After collection, all samples were kept at 37°C and were de-identified prior to delivery to the laboratory except for assignment of a unique identification number. Sample analysis was initiated after completion of liquefaction and within 1 h of ejaculation. At least 100 cells were assessed in each of two duplicates for determination of cell motility, viability and morphology, with at least 5 microscope fields of view being examined in each duplicate count. Sperm morphology was assessed in accordance with WHO criteria (World Health Organization, 2010) in the absence of papanicolaou, Shorr or Diff-Quik staining using 400 × magnification and bright field microscopy (Olympus CX40, Olympus, Sydney, Australia). Motility assessment was performed using phase contrast microscope optics (400 × magnification), with cells being classified as either motile (i.e. sperm that displayed any form of motility ranging from rapid progressive to non-progressive) or immotile. The aliquot of semen used for assessment of sperm concentration was sampled using a positive displacement pipette with care taken to avoid the introduction of bubbles during aspiration. No assessment of anti-sperm antibodies was performed, however all samples were free of abnormal clumping (aggregates and agglutinates) and the presence of excessive inflammatory cells (<1 million/ml). No biochemical markers for prostatic, seminal vesicle or epididymal secretions were analysed owing to our focus on spermatozoa.

**Human spermatozoa preparation and capacitation**

Human semen samples were fractionated over a discontinuous Percoll density gradient (comprising 40% and 80% Percoll suspensions) by centrifugation at 500 × g for 30 min (Redgrove *et al.*, 2012). After centrifugation, two fractions comprising the interface of the 40 and 80% Percoll suspensions and the pellet at the base of the 80% Percoll suspension were collected individually prior to being resuspended in a non-capacitating (non-cap) formulation of Biggers, Whitten and Whittingham medium (BWW) (Biggers *et al.*, 1971) containing 1 mg/ml polyvinyl alcohol (PVA) but prepared

without $HCO_3^-$(osmolarity of 290-310 mOsm/kg) (Bromfield *et al.*, 2015a). A subset of these cells were assessed for motility and concentration while the remainder were washed by centrifugation at 500 × g for 15 min. The sperm cells collected from the base of the 80% Percoll suspension are nominally referred as 'good quality' or 'mature' spermatozoa, whereas those partitioning at the 40 / 80% Percoll interface are referred to as 'poor quality' spermatozoa (Aitken *et al.*, 1993). Unless otherwise stated, good quality spermatozoa were used throughout our experiments following their resuspension in medium appropriate to experimental requirements.

To induce capacitation in vitro, spermatozoa were incubated in a formulation of BWW (91.5 mM NaCl, 4.6 mM KCl, 1.7 mM $CaCl_2.2H_2O$, 1.2 mM $KH_2PO_4$, 1.2 mM $MgSO_4.7H_2O$, 25 mM $NaHCO_3$, 5.6 mM D-glucose, 0.27 mM sodium pyruvate, 44 mM sodium lactate, 5 U/ml penicillin, 5 mg/ml streptomycin, 20 mM HEPES buffer, 1 mg/ml PVA (substituted for BSA; osmolarity of 290-310 mOsm/kg), 3 mM pentoxifylline and 5 mM dibutyryl cyclic adenosine monophosphate) that has previously been optimised for the induction of human sperm capacitation as assessed via tyrosine phosphorylation status, zona pellucida binding competence and, importantly in the context of this study, the ability to complete an acrosome reaction (Mitchell *et al.*, 2007). Where indicated, the capacitating medium was supplemented with either DMSO (vehicle control), Dynasore, Dyngo 4a or Dyngo-Ɵ. Spermatozoa were incubated at a concentration of $10 \times 10^6$ cells/ml at 37°C under an atmosphere of 5% $CO_2$:95% air for 3 h with a gentle inversion every 30 min to prevent settling of the cells (Mitchell *et al.*, 2007; 2008; Redgrove *et al.*, 2011). After incubation, spermatozoa were prepared for assessment of the capacity to undergo an acrosomal reaction utilising the assay protocols outlined below.

**Acrosomal reaction assays**

Following appropriate incubation, spermatozoa (non-capacitated, capacitated, dynamin inhibited or Dyngo-Ɵ treated) were induced to acrosomal react by supplementation of media with either 2.5 µM A23187 for 30 min, or 15 µM progesterone (pH 7.00 - 7.05) for 2 h in the presence of dynamin inhibitors or vehicle controls prepared at the same concentration as utilised during the initial

capacitation incubation. The spontaneous rates of acrosome loss were assessed via the inclusion of a capacitated sperm control group (designated Cap control), which were prepared under identical incubation conditions with the exception that they did not receive an A23187 or progesterone stimulus. At the completion of this induction period, sperm motility and viability were assessed (Bromfield *et al.*, 2015a) to ensure neither parameter was compromised by any of the treatments. The cells were then incubated in pre-warmed hypo-osmotic swelling media (HOS; 0.07% w/v sodium citrate; 1.3% w/v fructose) for another 30 min at 37°C. After being fixed in 4% PFA, spermatozoa were aliquoted onto 12-well slides, air-dried and permeabilised with ice cold methanol for 10 min. Cells were then incubated with FITC-conjugated PNA (1 µg/µl) at 37°C for 15 min, and the acrosomal status of viable cells (possessing coiled tails as a result of incubation in HOS medium) were verified using fluorescence microscopy (Zeiss Axio Imager A1, Jena, Thuringia, Germany). The wavelengths of the microscopic filters used for excitation and emission were 474 nm and ~527 nm.

**Immunofluorescent localisation**

Human testis and epididymis sections used in this study were kindly provided by Dr Zhuo Yu of Shanghai Jiaotong University. These tissues were collected from donors diagnosed with prostatic carcinoma but showing normal morphology of both the testis and epididymis. Tissues were fixed in fresh Bouin's solution, embedded in paraffin and sectioned at 5 µm thickness. Embedded tissue was dewaxed, rehydrated, and then subjected to antigen retrieval as previously reported (Zhou *et al.*, 2017). After being blocked with 3% BSA/PBS at 37°C for 1 h, slides were incubated with primary antibodies at 4°C overnight (for specific dilution rates of all antibodies please see Supplemental Table S1). After three washes in PBS, slides were incubated with appropriate Alexa Fluor conjugated secondary antibodies at 37°C for 1 h. Following additional washes, slides were incubated with PNA at 37°C for 15 min and counterstained with nuclear dyes; propidium iodide (5 µg/ml) or 4', 6-diamidino-2-phenylindole (2 µg/ml). Slides were then washed and mounted with a 10% Mowiol 4-88 with 30% glycerol in 0.2 M Tris (pH 8.5) and 2.5% 1, 4-diazabicyclo-(2.2.2)-

octane (DABCO). Staining patterns were recorded using fluorescence microscopy (Zeiss Axio Imager A1, Jena, Thuringia, Germany). The wavelengths of the microscopic filters used for excitation and emission were 474 nm and ~527 nm (Alexa Fluor 488 and propidium iodide), and 585 nm and ~615 nm (Alexa Fluor 594). Alternatively, confocal microscopy (Olympus IX81) was used for detection of fluorescent-labelling patterns using excitation and emission filters of wavelength 473 nm and 485–545 nm (Alexa Fluor 488), and 559 nm and 570–670 nm (propidium iodide).

For immunofluorescent staining of human spermatozoa, cells were fixed in 4% (w/v) PFA for 15 min at room temperature, washed in 0.05 M glycine/PBS and settled onto poly-L-lysine treated coverslips at 4°C overnight. For detection of the CDK1 kinase, cells were then subjected to antigen retrieval via immersion in 100 mM Tris, 5% urea (pH 9.5) at 90°C for 10 min (Reid *et al.*, 2015) and permeabilized with 0.1% Triton X-100 for 10 min. For detection of all other proteins, spermatozoa were permeabilized with ice cold methanol for 10 min (no antigen retrieval required). Following PBS washes, cells were blocked with 3% BSA/PBS and immunolabeled as described for human testis and epididymis slides.

**Electron microscopy**

Human spermatozoa were fixed in 4% (w/v) PFA containing 0.5% (v/v) glutaraldehyde. Cells were then processed via dehydration, infiltration and embedding in LR White resin. Sections (80 nm) were cut with a diamond knife (Diatome Ltd, Bienne, Switzerland) on an EM UC6 ultramicrotome (Leica Microsystems, Vienna, Austria) and placed on 200-mesh nickel grids. Subsequent washes were performed using PBS containing 1% fetal calf serum (FCS). After being blocked with 10% FCS + 1% cold water fish gelatin in PBS (30 min), sections were incubated with primary antibodies overnight at 4°C. An appropriate secondary antibody conjugated to 10 nm (anti-goat) gold particles was incubated on grids for 90 min at room temperature. Sections were counterstained in 2% (w/v) uranyl acetate. Micrographs were taken on a Tecnai 12 transmission electron microscope (FEI Company) at 120kV.

**SDS-PAGE and immunoblotting**

Protein was extracted from human spermatozoa via boiling in SDS extraction buffer (0.375M Tris pH 6.8, 2% w/v SDS, 10% w/v sucrose, protease inhibitor cocktail) at 100°C for 5 min. Insoluble material was removed by centrifugation (17,000 × g, 10 min, 4°C) and soluble protein remaining in the supernatant was quantified using a BCA protein assay kit (Thermo Fisher Scientific). Extracellular vesicles were isolated from seminal plasma using an optimised Optiprep density gradient protocol (Reilly *et al.*, 2016) and proteins were extracted and quantified as described for human sperm samples. Equivalent amounts of protein (10 µg) were boiled in SDS-PAGE sample buffer (2% v/v mercaptoethanol, 2% w/v SDS, and 10% w/v sucrose in 0.375 M Tris, pH 6.8, with bromophenol blue) at 100°C for 5 min, prior to be resolved by SDS-PAGE (150 V, 1 h) and transferred to nitrocellulose membranes (350 mA, 1 h). Similar protocols were also used in order to prepare human testis protein (sc-363781) for immunoblotting. Membranes were then blocked and incubated with appropriate antibodies raised against target proteins by using optimised conditions as previous described (Zhou *et al.*, 2017). Briefly, blots were washed three times × 10 min with either PBS supplemented with 0.5% (v/v) Tween-20 (PBST) (dynamin 1), or Tris-buffered saline with 0.1% (v/v) Tween-20 (TBST) (dynamin 2, dynamin 3, dynamin pSer778 and α-tubulin), before being probed with appropriate HRP-conjugated secondary antibodies (see Supplemental Table S1). After three additional further washes, labelled proteins were detected using an enhanced chemiluminescence kit (GE Healthcare). Where appropriate labelled protein band intensity was determined by densitometry using Image J-win64 software (Gassmann *et al.*, 2009; Xia *et al.*, 2016).

**Immunoprecipitation**

Capacitated spermatozoa were progesterone treated for 1 h. After treatment, cell lysis was performed on a total population of ~$100 \times 10^6$ cells in 200 µl cell lysis buffer (10 mM CHAPS, 10 mM HEPES, 137 mM NaCl and 10% glycerol supplemented with a protease inhibitor cocktail) at 4°C for 2 h. Following centrifugation (15,000 × g, 4°C for 10 min), the supernatant containing soluble protein was transferred to a clean tube and precleared by incubation with 50 µl aliquots of a

protein G Dynabead slurry at 4°C for 30 min. A total of 3 µg of anti-DNM2 antibody was then added to the precleared cell lysate followed by overnight incubation at 4°C with constant rotation. At the completion of this incubation period, protein G Dynabeads were added and the suspension returned to rotation for a further 30 min at 4°C to facilitate the precipitation of target antigens. The beads were subsequently washed three times in PBS, prior to resuspension in SDS loading buffer and boiling for 5 min to elute target proteins. These proteins were then subjected to immunoblotting with either anti-DNM2 or anti-DNM1 serine-778 antibodies.

**Duolink proximity ligation assay**

Human spermatozoa were prepared for Duolink in-situ proximity ligation assays (PLAs) as previously described. In brief, capacitated populations of human spermatozoa were incubated in the presence or absence of progesterone (15 µM) for 1 h. Non-capacitated cells were incubated for the same time period in non-cap BWW medium alone. Following incubation, sperm motility and viability were recorded and the cells were then fixed, washed and settled onto poly-L-lysine treated coverslips at 4°C overnight. After antigen retrieval and permeabilisation (see immunofluorescence; all antibodies used for PLA were first assessed via immunofluorescence for compatibility of antigen retrieval conditions), PLA labelling was conducted according to the manufacturers' instructions (OLINK Biosciences, Uppsala, Sweden) using pairs of primary antibodies comprising anti-CDK1 and anti-DNM2, anti-CDK1 and anti-DNM1 or anti-CDK1 and anti-IZUMO1 (irrelevant antibody control). Appropriate synthetic oligonucleotide-conjugated secondary antibodies (OLINK Biosciences) were subsequently applied for incubation at 37°C 1 h. After ligation and amplification, sperm cells were viewed using fluorescence microscopy (Zeiss Axio Imager A1). In this assay, target proteins residing within a maximum distance of 40 nm from each other are detected via the generation of foci of red fluorescent dots. A threshold of three or more fluorescent foci within the sperm head was set as for the recording of positive PLA signals (Bromfield *et al.*, 2015b). Using this criterion, a total of 100 spermatozoa were assessed per sample (n = 5) and the percentage of PLA positive cells was recorded.

### Statistics

Experiments reported in this study were repeated on at least five unique biological samples, with each sample representing semen collected from a single healthy normozoospermic donor. For the purpose of assessing acrosome reaction status and dynamin labelling profiles, ≥100 spermatozoa were counted in each sample and the corresponding percentage of acrosome reacted or positively labelled cells, respectively were determined dividing by the total number of cells counted. Graphical data are presented as the mean values ± SEM, which were calculated from the variance between samples. Statistical significance was determined by using an ANOVA.

## RESULTS

### Detection of dynamin isoforms in human testis and mature spermatozoa

The presence of the three canonical dynamin isoforms (DNM1, DNM2, and DNM3) was assessed in lysates prepared from human testis and ejaculated spermatozoa. For this purpose, testis lysate was purchased from a commercial source (Santa Cruz Biotechnology) and Percoll fractionated spermatozoa were isolated from the semen of at least five donors of known fertility. In the case of DNM1, a predominant band of the anticipated size (~100 kDa) was detected in the mature sperm lysate (Figure 1A). Notably however, an equivalent protein was not detected in human testis lysate (Figure 1A). To discount the possibility of protein degradation within the testis lysate, these samples were further assessed by stripping of the membranes and re-probing with anti-α-tubulin antibody. This approach confirmed both the integrity of the testis protein sample and the equivalent protein loading achieved between testis and sperm lysates. To address the alternative possibility of relatively low DNM1 expression in human testes, the quantity of testis protein was increased three fold (i.e. 30 µg versus 10 µg for sperm lysate) but there was no associated increase in the detection of DNM1 (data not shown).

The detection of a doublet of around 100 kDa for DNM1 in sperm lysates (Figure 1A, arrowheads) also prompted a further investigation of the potential for this band to represent a phosphorylated form of the protein. For this purpose, additional immunoblotting was conducted on the same homogenates of mouse brain (a tissue in which abundant phosphorylated DNM1 is present), and human spermatozoa using an antibody that detects phosphorylated DNM1 serine-778. Labelling with this antibody was restricted to the higher molecular weight band (Figure 1A, arrows) potentially indicating that the basal level of DNM1 phosphorylation differs depending on the tissue from which the protein is isolated.

Notwithstanding some minor cross-reactivity, dominant protein bands corresponding to those of the predicted size for DNM2 and DNM3 (also ~100 kDa) were detected in both the human testis and sperm lysates (Figures 1B and 1C, arrowheads). In all cases, an additional positive control consisting of mouse brain lysate was subsequently probed for DNM1, DNM2 and DNM3, revealing the labelling of the same size band in this tissue (Figure 1).

**Immunolocalisation of dynamin isoforms in human testis**

In view of the detection of dynamin expression in the human testis and/or sperm lysates, we next sought to investigate the specific localisation of these enzymes within histological sections of human testes. Immunofluorescence was applied in this study in combination with a peanut agglutinin (PNA) counterstain of the developing sperm acrosome (Mortimer *et al.*, 1987), and representative micrographs illustrating the expression patterns of dynamin are shown in Figure 2. Consistent with the immunoblotting of testis lysate, immunofluorescence failed to reveal any significant DNM1 expression in human testis sections (Figures 2A-C). The absence of DNM1 labelling persisted despite the application of a variety of antigen retrieval techniques in combination with trials to optimise incubation time and antibody concentration (data not shown). These data contrast those obtained for DNM2 immunolabelling, with distinct fluorescence foci being readily detected for DNM2 in the developing germ cell population of the human testes. While the quality of the testis sections precluded the precise determination of the temporal expression of DNM2,

spatially, the protein was clearly co-localised with PNA in round and elongating spermatids (Figures 2E-G). Such findings implicate DNM2 in acrosomal biogenesis during the later stages of the spermatogenic cycle. Additional DNM2 immunofluorescence was also detected, albeit considerably weaker, within the Sertoli cells of the seminiferous tubules. In the case of DNM3, a punctate pattern of localisation was observed throughout the seminiferous tubules and, whilst this labelling did appear in the vicinity of the developing germ cells (Figures 2I-K), we failed to detect any direct co-localisation of DNM3 and PNA in germ cell populations. These later findings agree with those reported in the mouse testis (Reid *et al.*, 2012), and suggest that DNM3, like that of DNM1, is unlikely to participate in the morphogenesis of the acrosomal vesicle in human spermatozoa. The specificity of all immunolabelling studies was confirmed through the inclusion of negative controls comprising secondary antibodies only (Figure 2D, H, L) and anti-dynamin antibodies that had been pre-absorbed with excess immunising peptide (where available, Supplementary Figure S1A). As anticipated, none of these controls revealed any labelling of testis sections.

**Immunolocalisation of dynamin isoforms in human spermatozoa**

Immunofluorescent localisation of dynamin was also performed on the isolated spermatozoa of normozoospermic donors (Figure 3). In order to account for the possibility of either inter- and intra-donor variability in dynamin expression, these studies were conducted on spermatozoa obtained from at least five different donors, as well as on the spermatozoa purified from multiple ejaculates obtained from the same donor, respectively. Among the notable findings from this analysis was the detection of strong DNM1 labelling throughout the entire spermatozoon (Figure 3A). Importantly, this pattern of localisation was present in virtually all cells examined, irrespective of whether they were sourced from multiple ejaculates of the same, or different, donors (Figures 3D and E). While such results clearly contrast those obtained in human testis sections (Figures 2A-C), they nevertheless accord with the positive DNM1 protein band labelled in human sperm lysates (Figure 1A). Since spermatozoa leaving the testis are incapable of either gene transcription or protein

translation, such findings raise the prospect that DNM1 may be acquired by spermatozoa from the external environment in which they are bathed during their functional maturation in the epididymis.

To begin to investigate this possibility, human epididymal sections were subjected to immunofluorescence labelling under identical conditions to those described for the testes. This analysis revealed positive DNM1 staining throughout the cytoplasm of the epithelial cells lining the epididymal duct (Supplementary Figure S2A). Additional labelling was also detected in the lumen of the epididymis and, at least a portion of this, was found to co-localise with sperm heads (Supplementary Figure S2A). Although we failed to source a reliable supply of human epididymal fluid, we were able to detect a positive signal for DNM1 by immunoblotting of whole seminal fluid (Supplementary Figure S2B). A similar DNM1 band was also present in fractionated seminal fluid samples prepared using an Optiprep density gradient protocol that has been optimised for the isolation of extracellular vesicles (Supplementary Figure S2B). While further experimentation is required before definitive conclusions can be drawn, such data offer tentative support for the delivery of DNM1 to maturing human spermatozoa during their post-testicular maturation.

Similar to DNM1, DNM2 was also readily detected in human spermatozoa. In this case however, the most common pattern of labelling placed DNM2 in the sperm head and the mid-piece of their flagellum, with essentially no labelling being detected in the principal-piece of the flagellum (Figures 3B, F and G). The labelling of DNM2 in the head was further verified by electron microscopy, which demonstrated positive immunogold labelling within the acrosomal domain (Supplementary Figure S3). In contrast with DNM2, only very weak DNM3 staining was recorded in human spermatozoa. In the majority of cells, this labelling appeared restricted to the mid-piece of the flagellum, but in approximately 20% of the population it was accompanied by additional labelling within the sperm head (Figures 3C, H and I). Such weak labelling of DNM3 raises the prospect that DNM1 and/or DNM2 fulfil the predominant functional role(s) of dynamin in mature spermatozoa. In all cases, dynamin labelling was highly reproducible and displayed minimal variation among the biological replicates examined. Similarly, the inclusion of negative controls in

which spermatozoa were incubated with either secondary antibodies only (Figure 3A-C, insets) or anti-dynamin antibodies that had been pre-absorbed with excess immunising peptide (where available, Supplementary Figure S1B) also supported the specificity of the immunofluorescent staining we documented across these samples.

**Inhibition of dynamin 1 and 2 suppresses the induction of acrosomal exocytosis in vitro**

The localisation of DNM1 and DNM2 in the anterior region of the head of mature human spermatozoa ideally positions these two isoforms to participate in the regulation of acrosomal exocytosis, consistent with the putative function of the enzymes in mouse spermatozoa (Reid *et al.*, 2012). We therefore investigated whether pharmacological inhibition of DNM1 and DNM2 could compromise the in-vitro induction of acrosomal exocytosis in human spermatozoa. However, prior to implementing these experiments, we first sought to optimise an assay capable of eliciting an acrosome reaction independent of the use of a calcium ionophore. For this purpose, capacitated populations of human spermatozoa were primed with progesterone during incubation in capacitating BWW media formulated to encompass the pH range of 6.4 to 7.8. Live cells were subsequently assessed for their acrosomal status by labelling with FITC-conjugated PNA, with those cells displaying curled tails (induced by incubation in HOS medium) and green fluorescence over the complete peri-acrosomal domain being classified as acrosome intact (Cheng *et al.*, 1996). In contrast, acrosome reacted spermatozoa were defined as those in which PNA was either absent or restricted to the equatorial domain (Cheng *et al.*, 1996; Esteves *et al.*, 1998). By imposing these criteria, we consistently achieved optimal acrosome reaction rates in BWW with a pH of 7.00 - 7.05 (Supplementary Figure S4).

Using these optimised conditions, populations of human spermatozoa were found to be significantly inhibited in their capacity to undergo a progesterone-induced acrosome reaction if capacitation medium was supplemented with the dynamin inhibitors of Dynasore or Dyngo 4a (Figure 4A, $P < 0.05$), compared to spermatozoa from the capacitated + vehicle (DMSO) control

group. The inclusion of Dyngo-Θ, an inactive chemical analogue of Dynasore and Dyngo 4a, did lead to a modest suppression of acrosome reaction rates. Importantly however, this reduction did not prove to be significantly different from that of either of the positive control treatment groups (capacitated ± DMSO), but did differ significantly ($P < 0.05$) compared to both Dynasore and Dyngo 4a groups, thus precluding the possibility of non-specific pharmacological inhibition.

The selectivity of inhibition was reinforced by the demonstration that neither Dynasore nor Dyngo 4a could prevent the induction of acrosomal exocytosis by the calcium ionophore, A23187. Indeed, no significant differences were recorded in levels of A23187 induced acrosome reaction rates among the capacitated populations of spermatozoa treated with either Dynasore, Dyngo 4a, Dyngo-Θ or DMSO (Figure 4B). Further, neither of the dynamin inhibitors nor the inactive isoform control had a detrimental impact on sperm viability, which consistently remained above 75% in all treatment groups. In the case of Dyngo 4a, we did record a modest reduction in overall sperm motility (Supplementary Figure S5). However, an equivalent reduction in sperm motility was not observed in the cells treated with Dynasore. Overall, these results are consistent with our previous reports of the response of mouse spermatozoa to dynamin inhibition (Reid *et al.*, 2012), indicating a conserved relationship between the activity of this enzyme and the ability of spermatozoa to undergo a progesterone-induced acrosome reaction.

**Comparison of dynamin expression in populations of good and poor quality human spermatozoa**

The ability to modulate acrosomal responsiveness in human spermatozoa through selective inhibition of dynamin prompted a more detailed evaluation of this enzyme in good and poor quality human sperm cells. To achieve this, semen samples from healthy normozoospermic individuals were fractionated via Percoll density gradient centrifugation into two discrete populations, referred to as a poor quality fraction (i.e. spermatozoa that partitioned at the interface of the 40-80% Percoll suspension) and a good quality fraction (i.e. high quality spermatozoa that pelleted at the base of 80%

Percoll suspension). These two populations of human spermatozoa have been well characterized in previous reports and shown to possess significant differences in morphology ($P < 0.03$), motility, and competence to fuse with the oolemma ($P < 0.001$) (Aitken *et al.*, 1993). The presence of contaminating cellular debris, immature germ cells and other components within the poor quality fraction precluded the use of immunoblotting to accurately determine the relative amount of the dynamin isoforms in each subpopulation of spermatozoa. Thus, immunofluorescence was applied with a view to determining the percentage of spermatozoa harbouring DNM1 and DNM2 within the anterior head.

As illustrated in Figures 5A and 5B, a similar proportion of spermatozoa displayed DNM1 head labelling irrespective of whether they were recovered from the poor or good quality subpopulations. In marked contrast, a dramatic underrepresentation of DNM2 was recorded in spermatozoa that partitioned into the lower quality subpopulation. Notably, this highly significant reduction in DNM2 labelling was restricted to the sperm head, with the majority of these cells retaining DNM2 labelling in the mid-piece of their flagellum (Figures 5C and D).

To begin to explore the functional consequences of reduced DNM2 expression in the head of poor quality spermatozoa, we compared the ability of our sub-populations to undergo an acrosome reaction in response to either a progesterone or calcium ionophore (A23187) stimulus. This analysis was again conducted using FITC-PNA labelling to assess acrosomal integrity and only live spermatozoa (possessing coiled tails as a result of incubation in HOS medium) were counted. Consistent with the reduction of DNM2 in the sperm head, those cells that were separated into the poor quality fraction proved entirely refractory to progesterone stimulus (Figure 5E). Notably, the highly significant diminution in the response of these poor quality cells occurred despite the apparent retention of DNM1 in the sperm head (Figures 5A and B). It also contrasted with the results obtained with the good quality sub-population, over 35% of which were induced to acrosome react following progesterone challenge (Figure 5E). Importantly, this lack of

responsiveness was restricted to progesterone-induced acrosome reactions, such that no equivalent decrease was observed following exposure to calcium ionophore (A23187) (Figure 5F).

**CDK1 regulates acrosomal reaction through dynamin phosphorylation**

It is well established that dynamin function is regulated through alternating cycles of phosphorylation/de-phosphorylation. We therefore sought to investigate if DNM1 and DNM2 activity in human spermatozoa is also regulated through phosphorylation. Specifically, we focused on the characterisation of CDKs (CDK1 and CDK5), serine/threonine kinases that reportedly target DNM2 Ser-764 and DNM1 Ser-778 for phosphorylation in somatic cells (Tan *et al.*, 2003; Chircop *et al.*, 2011). Through the use of immunofluorescence labelling, we found CDK1 was detected in the peri-acrosomal region of the human sperm head (Figure 6A). In contrast, CDK5 displayed a restricted profile of localisation within the mid-piece of the flagellum with no accompanying head labelling being detected irrespective of the functional status (non-capacitated, capacitated and progesterone treated) of the sperm samples analysed (Figure 6B illustrates the representative labelling detected in a non-capacitated spermatozoon). This raises the possibility of CDK1 targeting the substrates of DNM1 and/or DNM2 in the peri-acrosomal domain.

An in-situ proximity ligation assay (PLA) was therefore employed to assess the co-localisation of DNM1/DNM2 and CDK1 using the criterion of ≥3 punctate red fluorescent spots within the sperm head as a threshold for positive PLA labelling (Bromfield *et al.*, 2015b) (Figure 7). The combination of anti-CDK1 and anti-DNM2 antibodies, generated positive PLA signals that were primarily distributed over the anterior region of the sperm head. Although the percentage of CDK1/DNM2 PLA positive cells did not change following the induction of capacitation, it was significantly increased (from ~5% to ~30%, $P < 0.01$) upon the receipt of a progesterone stimulus. In contrast, minimal PLA labelling was detected for the combination of anti-CDK1 and anti-DNM1 antibodies irrespective of the functional status of the spermatozoa (Figure 7A, C and Supplementary Figure S6). Similarly, the irrelevant combination of anti-CDK1 and anti-IZUMO1 or anti-DNM1 and anti-BAG6 antibodies also failed to generate positive PLA signals (Figure 7B).

Having secured evidence for a putative interaction between CDK1 and DNM2, we next sought to investigate whether pharmacological inhibition of CDK1 could compromise phosphorylation of DNM2 and consequently result in reduced rates of acrosomal exocytosis following progesterone stimulation. Previous reports indicate that the dominant site for DNM2 phosphorylation site is the residue Ser-764, which is homologous to the phosphorylation site of Ser-778 in DNM1 (Chircop *et al.*, 2011). Thus, we treated human spermatozoa with 10 µM CDK1 inhibitor ($IC_{50}$= 5.8 µM; (Andreani *et al.*, 2000) prior to assessing DNM1 Ser-778/DNM2 Ser-764 phosphorylation status with an antibody (anti-DNM1 Ser-778) that also recognises the phosphorylated form of DNM2 Ser-764 residue (Supplementary Figure S7). As shown in Figures 8A and B, spermatozoa treated with the CDK1 inhibitor experienced a significant reduction in the levels of phosphorylated DNM1 Ser-778/DNM2 Ser-764. Importantly, this reduction in phospho-labelling was restricted to the sperm head, coinciding with the location of CDK1 (Supplementary Figure S8), and was not attributed to the loss of acrosomal contents, which were readily labelled with PNA in these spermatozoa (Figure 8C). (Loss of acrosomal contents has also been associated with loss of DNM1 Ser-778/DNM2 Ser-764 in the acrosomal region; Supplementary Figure S9). The impact of CDK1 inhibition also extended to a significant reduction in the rates of acrosomal exocytosis elicited in response to progesterone challenge (Figure 8D) compared to that of the vehicle control (DMSO) group. Taken together, these data implicate the necessity for dynamin phosphorylation in the regulatory control of human sperm acrosomal exocytosis.

## DISCUSSION

The completion of an acrosome reaction is a prerequisite for successful fertilisation and accordingly, failure to complete this unique exocytotic event represents a common aetiology underpinning the defective sperm function of infertile males (Muller, 2000; Liu and Baker, 2003). In support of recent studies implicating the dynamin family of mechanoenzymes as important regulators of the

acrosome reaction in murine spermatozoa (Reid *et al.*, 2012), we have provided evidence that this function may also be conserved in the spermatozoa of our own species. Specifically, our study has revealed that the canonical dynamin isoforms of DNM1, DNM2 and DNM3 are each represented among the proteome of ejaculated human spermatozoa. Further, DNM1 and DNM2 are ideally positioned within the anterior portion of the sperm head to enable them to exert an important regulatory influence over the acrosomal status of human spermatozoa. Accordingly, we report that the loss, or pharmacological inhibition of this enzyme, is associated with a concomitant reduction in the ability of human spermatozoa to complete a progesterone-induced acrosome reaction. The selectivity of such inhibition was supported by absence of an equivalent impact on acrosomal exocytosis induced by the calcium ionophore, A23187, which has the ability to bypass key physiological mechanisms required for acrosomal exocytosis (Buffone *et al.*, 2014).

The presence of dynamin isoforms within human spermatozoa has previously been recorded among the inventories arising from large scale proteomic profiling studies of fertile donors (Wang *et al.*, 2013; Amaral *et al.*, 2014). Indeed, these studies have revealed that human sperm harbour dynamin 2 and 3, in addition to the dynamin-like isoforms such as dynamin 1 like protein, dynamin like 120 kDa protein S1. However, to the best of our knowledge, our study represents the first to confirm the presence of the three canonical dynamin isoforms and report their spatial expression profiles in the human testis, epididymis and ejaculated spermatozoa. Our findings raise the prospect that this family of mechanoenzymes may fulfil diverse, yet evolutionary conserved roles in the support of male germ cell development and function. Notwithstanding this possibility, we also observed some variation in the expression patterns of dynamin isoforms, anticipated on the basis of previous observations in rodent models.

One particular curiosity was our inability to detect appreciable levels of dynamin 1 in human testis sections despite the relatively strong labelling of the protein in ejaculated spermatozoa (confirmed by both immunofluorescence and immunoblotting). Among the possible explanations for this observation is that DNM1 is either unmasked, or alternatively, uniquely acquired during the

post-testicular maturation of spermatozoa. Arguing against the former explanation is the fact that we were unable to detect DNM1 in testis sections despite the application of a variety of antigen retrieval steps that have previously been successfully implemented in the mouse (Zhou *et al.*, 2017). Further, transcript and protein expression data sourced from public databases (Gene Expression Omnibus profile and the European Bioinformatics Institute) also indicate that DNM1 is not expressed in the human testes. On the other hand, the tenet that DNM1 may be transferred to maturing spermatozoa draws on a wealth of evidence that the sperm proteome is substantially modified during their transit of the epididymis (Dacheux *et al.*, 2006; 2016; Sullivan and Mieusset, 2016). One of the principle mechanisms implicated in this form of intercellular communication is the interaction formed between spermatozoa and a population of extracellular vesicles, known as epididymosomes, which are secreted into the epididymal lumen (Sullivan, 2015). In support of this mechanism, we detected DNM1 in whole seminal fluid as well as an extracellular vesicle fraction isolated from this material. While the validity of this model of DNM1 acquisition awaits further investigation, the labelling of the protein in the peri-acrosomal domain of ejaculated spermatozoa suggests that it may work in tandem with DNM2, which occupies a similar location, to regulate the release of the acrosomal contents during a progesterone-induced acrosome reaction. Such functional redundancy is a relatively common feature of dynamin expression in somatic cells (Altschuler *et al.*, 1998), and is also commensurate with the overall importance of the acrosome reaction in terms of securing successful fertilisation.

Notwithstanding the potential for overlapping function between DNM1 and DNM2, our collective data lead us to conclude that DNM2 is likely to fulfil the dominant role in terms of both male germ cell development and function. Indeed, the conditional ablation of this ancestral form of the enzyme, which is most closely related to the dynamin-like proteins detected in lower organisms (Chircop *et al.*, 2011), leads to a complete arrest of early germ cell development (Redgrove *et al.*, 2016). In contrast, the loss of DNM1 at a similar stage of germ cell development had no discernible effect on either germ cell development or the fertility of the null males (Redgrove *et al.*, 2016). It is

also noted that during latter phases of germ cell development, the DNM2 protein co-localises with PNA at a time when Golgi-derived vesicles begin to fuse to form a single large secretory vesicle that eventually gives rise to the acrosome (Kierszenbaum *et al.*, 2003). This agrees with data implicating DNM2 as a key regulator of newly formed vesicles and post-Golgi vesicle exocytosis in various somatic cell types (Jones *et al.*, 1998; Kreitzer *et al.*, 2000; Grimmer *et al.*, 2005; Kessels *et al.*, 2006; Jaiswal *et al.*, 2009). On the basis of similar patterns of localisation in human testis, it is tempting to suggest that DNM2 may fulfil an equivalent role in our species. In a similar vein, the expression of DNM2 detected within the epididymal epithelium suggests that the protein may also exert an influence over the secretion of proteins into the epididymal lumen and, in so doing, influence the maturation of spermatozoa (Zhou *et al.*, 2017).

The possibility that such functional conservation extends to the control of mature human spermatozoa is supported by selective pharmacological inhibition, which led to a significant reduction in the ability of these cells to complete an acrosome reaction. However, in seeking to discern the relative importance of DNM1 and DNM2 in this response, it is notable that the dynamin inhibitors employed in this study target both isoforms with equivalent efficacy owing to their selective inhibition of the GTPase activity of these enzymes (Macia *et al.*, 2006; McCluskey *et al.*, 2013). Despite this, the importance of DNM2 is underscored by the dramatic underrepresentation of this isoform, but not DNM1, in the sub-population of poor quality spermatozoa recovered from healthy donors following density gradient centrifugation. Importantly, the apparent loss of DNM2 was correlated with reduced ability of these cells to complete a progesterone-induced acrosome reaction. The fact that these cells retained the competence to complete a calcium ionophore induced acrosome reaction, which is relatively forgiving of the functional status of the cell, indicates that this was not associated with compromised structural integrity of the acrosomal vesicle. While such findings would clearly benefit from further validation across an expanded cohort of patients with zona pellucida penetration defects, they nevertheless support the importance of the DNM2 in governing the acrosomal responsiveness of human spermatozoa.

An important caveat to this interpretation is that the putative importance of progesterone as a physiologically relevant stimulus to prime human spermatozoa for induction of acrosomal exocytosis remains the subject of active debate (Buffone *et al.*, 2014). Recent evidence mounts a compelling case in favour of this hypothesis by revealing that progesterone can interact either directly (Lishko et al., 2011; Strünker et al., 2011), or indirectly with CATSPER channels in human spermatozoa (Miller *et al.*, 2016). In the latter model, it is suggested that progesterone binds to abhydrolase domain containing 2 (ABHD2). This lipid hydrolase is highly expressed in human spermatozoa where it is responsible for the degradation of endocannabinoid 2-arachidonoylglycerol (2AG), and hence its depletion from the plasma membrane. Since 2AG inhibits CATSPER, its progesterone-dependent removal (Miller et al., 2016) serves to modulate intracellular calcium levels as necessitated for the induction of acrosomal exocytosis (Beltrán *et al.*, 2016). However, the fact that both CATSPER channels and ABHD2 are restricted to the flagellum of human spermatozoa (Lishko *et al.*, 2011; Strünker *et al.*, 2011; Miller *et al.*, 2016) raises the question of whether the CATSPER initiated calcium fluxes could be propagated to the anterior region of the sperm head. Tentative support for this model rests with the demonstration that mouse spermatozoa challenged with solubilised ZP proteins responded via the propagation of a CATSPER-dependent calcium wave that progressed from the flagellum toward the head (Ren and Xia, 2010). An alternative possibility is that progesterone could induce acrosomal exocytosis via interaction with progesterone receptors (Aquila and De Amicis, 2014) that are known to be located in the mid-piece/neck region of human spermatozoa (Thomas *et al.*, 2009). A further consideration is the prospect that the spermatozoa of different species may respond differently to progesterone stimulus. For instance, unlike their human counterparts, the CATPSER harbored by mouse spermatozoa is reportedly refractory to progesterone stimulus. Similarly, 2AG is removed from the plasma membrane of mouse spermatozoa prior to their completion of epididymal transit (Miller *et al.*, 2016). Despite this, mouse spermatozoa do retain the capacity to respond to progesterone through induction of an acrosome reaction (Osman *et al.*, 1989).

Irrespective of the pathways employed, our data emphasize the importance of downstream events tied to progesterone stimulus via the demonstration that dynamin phosphorylation can promote the induction of acrosomal exocytosis in the spermatozoa both humans and mice. Indeed, in our hands progesterone challenge led to an increase in phosphorylation of DNM1 Ser-778/DNM2 Ser-764 in human spermatozoa. The consequences of the phosphorylation of these dynamin residues has been studied extensively in the context of membrane remodelling and vesicle scission in somatic cells. In neural tissue, replacement of DNM1 and DNM3 with DNM1 dephospho- or phospho-mimetic mutations can either accelerate or decelerate the endocytotic process (Armbruster *et al.*, 2013). Similarly, DNM2 phosphorylation in endothelial cells has proven to be essential for scission of caveolae (Shajahan *et al.*, 2004). In our own studies, we have previously reported a substantive increase in dynamin phosphorylation in the peri-acrosomal region of mouse spermatozoa following progesterone challenge (Reid *et al.*, 2012). On the basis of these data we hypothesised that dynamin phosphorylation may slow the rate of expansion and/or stabilise the formation of fusion pores between the outer acrosomal membrane and plasma membrane thereby prolonging the exocytosis process consistent with the protracted kinetics of this unique secretory process. Our data from this study suggest that dynamin phosphorylation may also play a pivotal role in the modulation of its function in human spermatozoa. Further work is now needed to reconcile the differences in progesterone action in the spermatozoa of these two species.

In order to initiate these studies, we sought to identify the kinase responsible for dynamin phosphorylation, with our data revealing that CDK1 is a likely candidate in the phosphorylation of DNM2, but not DNM1, within the acrosomal region of progesterone stimulated spermatozoa. This result is consistent with independent studies identifying CDK1 as the principle kinase responsible for DNM2 phosphorylation in somatic cells and in mouse germ cells (Chircop *et al.*, 2011; Ferguson and De Camilli, 2012; Redgrove *et al.*, 2016). While we sought to confirm the CDK1 / DNM2 interaction using reciprocal co-immunoprecipitation, regrettably this interaction proved recalcitrant to this strategy irrespective of whether CDK1 or DNM2 were used as the bait. Among

the possible explanations, we consider that the transient nature of the kinase/substrate interaction, which is typically measured in milliseconds, precluded the capture of this event. Nevertheless, we did confirm that CDK1 co-localises with DNM2 in the anterior region of the sperm head and that the selective inhibition of this kinase suppressed the ability of these cells to respond to progesterone challenge in terms of both DNM2 phosphorylation (at Ser-764) and acrosomal exocytosis. In accounting for these findings, it is noteworthy that dynamin phosphorylation is known to regulate the enzymes GTPase activity and hence the scission of vesicles in neuronal tissues (Robinson *et al.*, 1993). These findings encourage speculation of a causative link between the suppression of DNM2 Ser-764 phosphorylation and the GTPase-dependent conformational change in the protein that putatively regulates acrosomal exocytosis. However, we are cognisant that CDK1 has the potential to phosphorylate multiple substrates (Ubersax *et al.*, 2003) and we remain uncertain what, if any, role(s) these additional targets have in the regulation of sperm function; thus, these data must be interpreted with caution.

In summary, the collective findings described in this, and our preceding studies of dynamin function, lead us to propose that this family of mechanoenzymes may hold conserved roles in the regulation of several aspects of male fertility. Chief among these are the support of acrosome formation during germ cell development and the regulated exocytotic release of the acrosomal contents that precedes fertilisation. Such activity appears to be intimately tied to the phosphorylation status of the protein, with our current study identifying CDK1 as a key regulatory kinase in the phosphorylation of DNM2. Our study has also provided evidence that the underrepresentation of DNM2 is associated with poor quality spermatozoa that fail to complete acrosomal exocytosis. Although the causative nature of these phenomenon awaits further investigation, this study stimulates further research into the potential of dynamin as a novel molecular target to assist with diagnosis of male infertility and the establishment of discrete criteria for the stratification of infertility patients into appropriate therapeutic options.

## Acknowledgements

The authors are grateful to Jodie Powell for orchestrating the panel of healthy donors used in this research and Dr Zhuo Yu of Shanghai Jiaotong University for the supply of human testis and epididymis sections.

## Authors' roles

W.Z. conducted the experiments and generated the manuscript. A.L.A provided technical assistance. A.P.T conducted the electron microscopy experiment. G.N.D and E.A.M contributed to study conception and design, data interpretation and manuscript editing. A.M provided Dyngo-Ɵ, the instruction of the usage of dynamin inhibitors. B.N conceived this study and contributed to study design, data interpretation, and manuscript preparation. All authors approved the final version and submission of this article.

## Funding

This research was supported by a National Health and Medical Research Council of Australia Project Grant (APP1103176) awarded to B.N. and E.A.M.

## Conflict of interest

The authors declare that they have no conflicts of interest.

## REFERENCES

Aitken RJ, Harkiss D, Buckingham D. Relationship between iron-catalysed lipid peroxidation potential and human sperm function. *J Reprod Fertil* 1993;**98**:257-265.

Aitken RJ, Nixon B. Sperm capacitation: a distant landscape glimpsed but unexplored. *Mol Hum Reprod* 2013;**19**:785-793.

Altschuler Y, Barbas SM, Terlecky LJ, Tang K, Hardy S, Mostov KE, Schmid SL. Redundant and distinct functions for dynamin-1 and dynamin-2 isoforms. *J Cell Biol* 1998;**143**:1871-1881.

Amaral A, Castillo J, Ramalho-Santos J, Oliva R. The combined human sperm proteome: cellular pathways and implications for basic and clinical science. *Hum Reprod Update* 2014;**20**:40-62.

Anantharam A, Bittner MA, Aikman RL, Stuenkel EL, Schmid SL, Axelrod D, Holz RW. A new role for the dynamin GTPase in the regulation of fusion pore expansion. *Mol Biol Cell* 2011;**22**:1907-1918.

Andreani A, Cavalli A, Granaiola M, Leoni A, Locatelli A, Morigi R, Rambaldi M, Recanatini M, Garnier M, Meijer L. Imidazo [2, 1-b] thiazolylmethylene-and indolylmethylene-2-indolinones: a new class of cyclin-dependent kinase inhibitors. Design, synthesis, and CDK1/cyclin B inhibition. *Anti-Cancer Drug Des* 2000;**15**:447-452.

Antonny B, Burd C, De Camilli P, Chen E, Daumke O, Faelber K, Ford M, Frolov VA, Frost A, Hinshaw JE. Membrane fission by dynamin: what we know and what we need to know. *EMBO J* 2016;**35**:2270-2284.

Aquila S, De Amicis F. Steroid receptors and their ligands: effects on male gamete functions. *Exp Cell Res* 2014;**328**:303-313.

Armbruster M, Messa M, Ferguson SM, De Camilli P, Ryan TA. Dynamin phosphorylation controls optimization of endocytosis for brief action potential bursts. *eLife* 2013;**2**:e00845.

Avella MA, Dean J. Fertilization with acrosome-reacted mouse sperm: Implications for the site of exocytosis. *Proc Natl Acad Sci* 2011;**108**:19843-19844.

Baibakov B, Gauthier L, Talbot P, Rankin TL, Dean J. Sperm binding to the zona pellucida is not sufficient to induce acrosome exocytosis. *Development* 2007;**134**:933-943.

Barros C, Bedford JM, Franklin LE, Austin CR. Membrane vesiculation as a feature of the mammalian acrosome reaction. *J Cell Biol* 1967;**34**:C1-5.

Belmonte SA, Mayorga LS, Tomes CN. The Molecules of Sperm Exocytosis (eds) *Sperm Acrosome Biogenesis and Function During Fertilization*. 2016. Springer, pp. 71-92.

Beltrán C, Treviño CL, Mata-Martínez E, Chávez JC, Sánchez-Cárdenas C, Baker M, Darszon A. Role of Ion Channels in the Sperm Acrosome Reaction (eds). *Sperm Acrosome Biogenesis and Function During Fertilization*. 2016. Springer, pp. 35-69.

Biggers JD, Whitten WK, Whittingham DG. Culture of mouse embryos in vitro. *In Methods in Mammalian Embryology* 1971:86-116.

Björndahl L, Barratt CL, Mortimer D, Jouannet P. 'How to count sperm properly': checklist for acceptability of studies based on human semen analysis. *Hum Reprod* 2015;**31**:227-232.

Blackmore PF, Beebe SJ, Danforth DR, Alexander N. Progesterone and 17 alpha-hydroxyprogesterone. Novel stimulators of calcium influx in human sperm. *J Biol Chem* 1990;**265**:1376-1380.

Bromfield EG, Aitken RJ, Anderson AL, McLaughlin EA, Nixon B. The impact of oxidative stress on chaperone-mediated human sperm–egg interaction. *Hum Reprod* 2015a;**30**:2597-2613.

Bromfield EG, Aitken RJ, Nixon B. Novel characterization of the HSPA2-stabilizing protein BAG6 in human spermatozoa. *Mol Hum Reprod* 2015b;**21**:755-769.

Buffone MG, Hirohashi N, Gerton GL. Unresolved questions concerning mammalian sperm acrosomal exocytosis. *Biol Reprod* 2014;**90**:1-8.

Buffone MG, Ijiri TW, Cao W, Merdiushev T, Aghajanian HK, Gerton GL. Heads or tails? Structural events and molecular mechanisms that promote mammalian sperm acrosomal exocytosis and motility. *Mol Reprod Dev* 2012;**79**:4-18.

Cao H, Garcia F, McNiven MA. Differential distribution of dynamin isoforms in mammalian cells. *Mol Biol Cell* 1998;**9**:2595-2609.

Cheng FP, Fazeli A, Voorhout WF, Marks A, Bevers MM, Colenbrander B. Use of Peanut Agglutinin to Assess the Acrosomal Status and the Zona Pellucida‐Induced Acrosome Reaction in Stallion Spermatozoa. *J Androl* 1996;**17**:674-682.

Chircop M, Sarcevic B, Larsen MR, Malladi CS, Chau N, Zavortink M, Smith CM, Quan A, Anggono V, Hains PG. Phosphorylation of dynamin II at serine-764 is associated with cytokinesis. *Biochim Biophys Acta* 2011;**1813**:1689-1699.

Cook TA, Urrutia R, McNiven MA. Identification of dynamin 2, an isoform ubiquitously expressed in rat tissues. *Proc Natl Acad Sci* 1994;**91**:644-648.

Dacheux JL, Belghazi M, Lanson Y, Dacheux F. Human epididymal secretome and proteome. *Mol Cell Endocrinol* 2006;**250**:36-42.

Dacheux JL, Dacheux F, Druart X. Epididymal protein markers and fertility. *Anim Reprod Sci* 2016;**169**:76-87.

Esteves SC, Sharma RK, Thomas AJ, Agarwal A. Cryopreservation of human spermatozoa with pentoxifylline improves the post-thaw agonist-induced acrosome reaction rate. *Hum Reprod* 1998;**13**:3384-3389.

Ferguson SM, Brasnjo G, Hayashi M, Wölfel M, Collesi C, Giovedi S, Raimondi A, Gong LW, Ariel P, Paradise S. A selective activity-dependent requirement for dynamin 1 in synaptic vesicle endocytosis. *Science* 2007;**316**:570-574.

Ferguson SM, De Camilli P. Dynamin, a membrane-remodelling GTPase. *Nat Rev Mol Cell Biol* 2012;**13**:75-88.

Florman HM, Jungnickel MK, Sutton KA. Regulating the acrosome reaction. *Int J Dev Biol* 2004;**52**:503-510.

Gassmann M, Grenacher B, Rohde B, Vogel J. Quantifying Western blots: pitfalls of densitometry. *Electrophoresis* 2009;**30**:1845-1855.

Grimmer S, Ying M, Wälchli S, van Deurs B, Sandvig K. Golgi Vesiculation Induced by Cholesterol Occurs by a Dynamin‐and cPLA2‐Dependent Mechanism. *Traffic* 2005;**6**:144-156.

Iguchi H, Watanabe M, Kamitani A, Nagai A, Hosoya O, Tsutsui K, Kumon H. Localization of dynamin 2 in rat seminiferous tubules during the spermatogenic cycle. *Acta Med Okayama* 2002;**56**:205-209.

Inoue N, Satouh Y, Ikawa M, Okabe M, Yanagimachi R. Acrosome-reacted mouse spermatozoa recovered from the perivitelline space can fertilize other eggs. *Proc Natl Acad Sci* 2011;**108**:20008-20011.

Jackson J, Papadopulos A, Meunier FA, McCluskey A, Robinson PJ, Keating DJ. Small molecules demonstrate the role of dynamin as a bi-directional regulator of the exocytosis fusion pore and vesicle release. *Mol Psychiatry* 2015;**20**:810-819.

Jaiswal JK, Rivera VM, Simon SM. Exocytosis of post-Golgi vesicles is regulated by components of the endocytic machinery. *Cell* 2009;**137**:1308-1319.

Jones SM, Howell KE, Henley JR, Cao H, McNiven MA. Role of dynamin in the formation of transport vesicles from the trans-Golgi network. *Science* 1998;**279**:573-577.

Kessels MM, Dong J, Leibig W, Westermann P, Qualmann B. Complexes of syndapin II with dynamin II promote vesicle formation at the trans-Golgi network. *J Cell Sci* 2006;**119**:1504-1516.

Kierszenbaum AL, Rivkin E, Tres LL. Acroplaxome, an F-actin–keratin-containing plate, anchors the acrosome to the nucleus during shaping of the spermatid head. *Mol Biol Cell* 2003;**14**:4628-4640.

Kreitzer G, Marmorstein A, Okamoto P, Vallee R, Rodriguez-Boulan E. Kinesin and dynamin are required for post-Golgi transport of a plasma-membrane protein. *Nat Cell Biol* 2000;**2**:125-127.

Kusumi N, Watanabe M, Yamada H, Li SA, Kashiwakura Y, Matsukawa T, Nagai A, Nasu Y, Kumon H, Takei K. Implication of amphiphysin 1 and dynamin 2 in tubulobulbar complex formation and spermatid release. *Cell struct Funct* 2007;**32**:101-113.

Lie PP, Xia W, Wang CQ, Mruk DD, Yan HH, Wong CH, Lee WM, Cheng CY. Dynamin II interacts with the cadherin-and occludin-based protein complexes at the blood–testis barrier in adult rat testes. *J Endocrinol* 2006;**191**:571-586.

Lishko PV, Botchkina IL, Kirichok Y. Progesterone activates the principal Ca2+ channel of human sperm. *Nature* 2011;**471**:387-391.

Liu DY, Baker HW. Disordered zona pellucida–induced acrosome reaction and failure of in vitro fertilization in patients with unexplained infertility. *Fertil Steril* 2003;**79**:74-80.

Macia E, Ehrlich M, Massol R, Boucrot E, Brunner C, Kirchhausen T. Dynasore, a cell-permeable inhibitor of dynamin. *Dev Cell* 2006;**10**:839-850.

McCluskey A, Daniel JA, Hadzic G, Chau N, Clayton EL, Mariana A, Whiting A, Gorgani NN, Lloyd J, Quan A. Building a better dynasore: the dyngo compounds potently inhibit dynamin and endocytosis. *Traffic* 2013;**14**:1272-1289.

Meizel S, Turner KO, Nuccitelli R. Progesterone triggers a wave of increased free calcium during the human sperm acrosome reaction. *Dev Biol* 1997;**182**:67-75.

Meyers SA, Overstreet JW, Liu IK, Drobnis EZ. Capacitation in vitro of stallion spermatozoa: comparison of progesterone-induced acrosome reactions in fertile and subfertile males. *J Androl* 1995;**16**:47-54.

Miller MR, Mannowetz N, Iavarone AT, Safavi R, Gracheva EO, Smith JF, Hill RZ, Bautista DM, Kirichok Y, Lishko PV. Unconventional endocannabinoid signaling governs sperm activation via the sex hormone progesterone. *Science* 2016;**352**:555-559.

Mitchell LA, Nixon B, Aitken RJ. Analysis of chaperone proteins associated with human spermatozoa during capacitation. *Mol Hum Reprod* 2007;**13**:605-613.

Mitchell LA, Nixon B, Baker MA, Aitken RJ. Investigation of the role of SRC in capacitation-associated tyrosine phosphorylation of human spermatozoa. *Mol Hum Reprod* 2008;**14**:235-243.

Morlot S, Roux A. Mechanics of dynamin-mediated membrane fission. *Annu Rev Biophys* 2013;**42**:629-649.

Mortimer D, Curtis EF, Miller RG. Specific labelling by peanut agglutinin of the outer acrosomal membrane of the human spermatozoon. *J Reprod Fertil* 1987;**81**:127-135.

Muller CH. Rationale, interpretation, andrology lab corner validation, and uses of sperm function tests. *J Androl* 2000;**21**:10-30.

Nixon B, MacIntyre DA, Mitchell LA, Gibbs GM, O'Bryan M, Aitken RJ. The identification of mouse sperm-surface-associated proteins and characterization of their ability to act as decapacitation factors. *Biol Reprod* 2006;**74**:275-287.

Osman RA, Andria ML, Jones AD, Meizel S. Steroid induced exocytosis: the human sperm acrosome reaction. *Biochem Biophys Res Commun* 1989;**160**:828-833.

Redgrove KA, Anderson AL, Dun MD, McLaughlin EA, O'Bryan MK, Aitken RJ, Nixon B. Involvement of multimeric protein complexes in mediating the capacitation-dependent binding of human spermatozoa to homologous zonae pellucidae. *Dev Biol* 2011;**356**:460-474.

Redgrove KA, Bernstein IR, Pye VJ, Mihalas BP, Sutherland JM, Nixon B, McCluskey A, Robinson PJ, Holt JE, McLaughlin EA. Dynamin 2 is essential for mammalian spermatogenesis. *Sci Rep* 2016;**6**.

Redgrove KA, Nixon B, Baker MA, Hetherington L, Baker G, Liu DY, Aitken RJ. The molecular chaperone HSPA2 plays a key role in regulating the expression of sperm surface receptors that mediate sperm-egg recognition. *PLoS One* 2012;**7**:e50851.

Reid AT, Anderson AL, Roman SD, McLaughlin EA, McCluskey A, Robinson PJ, Aitken RJ, Nixon B. Glycogen synthase kinase 3 regulates acrosomal exocytosis in mouse spermatozoa via dynamin phosphorylation. *FASEB J* 2015;**29**:2872-2882.

Reid AT, Lord T, Stanger SJ, Roman SD, McCluskey A, Robinson PJ, Aitken RJ, Nixon B. Dynamin regulates specific membrane fusion events necessary for acrosomal exocytosis in mouse spermatozoa. *J Biol Chem* 2012;**287**:37659-37672.

Reilly JN, McLaughlin EA, Stanger SJ, Anderson AL, Hutcheon K, Church K, Mihalas BP, Tyagi S, Holt JE, Eamens AL. Characterisation of mouse epididymosomes reveals a complex profile of microRNAs and a potential mechanism for modification of the sperm epigenome. *Sci Rep* 2016;**6**.

Ren D, Xia J. Calcium signaling through CatSper channels in mammalian fertilization. *Physiology* 2010;**25**:165-175.

Robinson PJ, Sontag JM, Liu JP, Fykse EM, Slaughter C, McMahontt H, Südhof TC. Dynamin GTPase regulated by protein kinase C phosphorylation in nerve terminals. *Nature* 1993;**365**:163-166.

Shajahan AN, Timblin BK, Sandoval R, Tiruppathi C, Malik AB, Minshall RD. Role of Src-induced dynamin-2 phosphorylation in caveolae-mediated endocytosis in endothelial cells. *J Biol Chem* 2004;**279**:20392-20400.

Shpetner HS, Vallee RB. Identification of dynamin, a novel mechanochemical enzyme that mediates interactions between microtubules. *Cell* 1989;**59**:421-432.

Stival C, Molina LdCP, Paudel B, Buffone MG, Visconti PE, Krapf D. Sperm Capacitation and Acrosome Reaction in Mammalian Sperm (eds). *Sperm Acrosome Biogenesis and Function During Fertilization*. 2016. Springer, pp. 93-106.

Strünker T, Goodwin N, Brenker C, Kashikar ND, Weyand I, Seifert R, Kaupp UB. The CatSper channel mediates progesterone-induced Ca2+ influx in human sperm. *Nature* 2011;**471**:382-386.

Sullivan R. Epididymosomes: Role of extracellular microvesicles in sperm maturation. *Front Biosci (Schol Ed)* 2015;**8**:106-114.

Sullivan R, Mieusset R. The human epididymis: its function in sperm maturation. *Hum Reprod Update* 2016;**22**:574-587.

Tan TC, Valova VA, Malladi CS, Graham ME, Berven LA, Jupp OJ, Hansra G, McClure SJ, Sarcevic B, Boadle RA. Cdk5 is essential for synaptic vesicle endocytosis. *Nat Cell Biol* 2003;**5**:701-710.

Thérien I, Manjunath P. Effect of progesterone on bovine sperm capacitation and acrosome reaction. *Biol Reprod* 2003;**69**:1408-1415.

Thomas P, Tubbs C, Garry VF. Progestin functions in vertebrate gametes mediated by membrane progestin receptors (mPRs): identification of mPRα on human sperm and its association with sperm motility. *Steroids* 2009;**74**:614-621.

Ubersax JA, Woodbury EL, Quang PN, Paraz M, Blethrow JD, Shah K, Shokat KM, Morgan DO. Targets of the cyclin-dependent kinase Cdk1. *Nature* 2003;**425**:859-864.

Vaid KS, Guttman JA, Babyak N, Deng W, McNiven MA, Mochizuki N, Finlay BB, Vogl AW. The role of dynamin 3 in the testis. *J Cell Physiol* 2007;**210**:644-654.

Visconti PE, Krapf D, de la Vega-Beltrán JL, Acevedo JJ, Darszon A. Ion channels, phosphorylation and mammalian sperm capacitation. *Asian J Androl* 2011;**13**:395-405.

Wang G, Guo Y, Zhou T, Shi X, Yu J, Yang Y, Wu Y, Wang J, Liu M, Chen X. In-depth proteomic analysis of the human sperm reveals complex protein compositions. *J Proteomics* 2013;**79**:114-122.

Williams M, Kim K. From membranes to organelles: emerging roles for dynamin-like proteins in diverse cellular processes. *Eur J Cell Biol* 2014;**93**:267-277.

World Health Organization. *WHO laboratory manual for the examination and processing of human semen Fifth edition*. 2010. Switzerland.

Xia Q, Chesi A, Manduchi E, Johnston BT, Lu S, Leonard ME, Parlin UW, Rappaport EF, Huang P, Wells AD. The type 2 diabetes presumed causal variant within TCF7L2 resides in an element that controls the expression of ACSL5. *Diabetologia* 2016;**59**:2360-2368.

Zhao L, Shi X, Li L, Miller DJ. Dynamin 2 associates with complexins and is found in the acrosomal region of mammalian sperm. *Mol Reprod Dev* 2007;**74**:750-757.

Zhou W, De Iuliis GN, Turner AP, Reid AT, Anderson AL, McCluskey A, McLaughlin EA, Nixon B. Developmental expression of the dynamin family of mechanoenzymes in themouse epididymis. *Biol Reprod* 2017;**96**:159-173.

## FIGURE LEGENDS

**FIGURE 1. Identification of dynamin isoforms in human testis and sperm lysates.** Human testis and sperm lysates were analysed for the presence of (**A**) dynamin 1 (DNM1), (**B**) dynamin 2 (DNM2), and (**C**) dynamin 3 (DNM3) using standard immunoblotting protocols. Mouse brain tissue homogenates were resolved alongside the human samples as a positive control for dynamin expression. After initial dynamin labelling, blots were stripped and re-probed with anti-α-tubulin antibody to confirm equivalent protein loading of each sample. (**A**) The detection of a doublet of approximately 100 kDa for DNM1 (arrowheads) prompted a further investigation of the potential for post-translational phosphorylation of this isoform. For this purpose, anti-phospho-DNM1-778 antibody was used to probe the same samples of mouse brain and human sperm lysates, revealing positive labelling of the higher molecular weight band (arrows). These experiments were repeated on spermatozoa obtained from five different healthy normozoospermic donors and representative

immunoblots are shown. In contrast, testicular lysates were obtained from a commercial supplier and represent material prepared from a single healthy donor.

**FIGURE 2. Immunofluorescence detection of dynamin isoforms within the human testis.** Antibodies against (**A**, **B**, and **C**) DNM1, (**D**, **E**, and **F**) DNM2, and (**G**, **H**, and **I**) DNM3 were used to determine the localisation of these proteins (red) in human testis sections. These sections were subsequently counterstained with PNA and DAPI to reveal the acrosome, and the cell nuclei (blue) of developing germ cells, respectively. For clarity, the structure of seminiferous tubules has been outlined. Among the three dynamin isoforms examined, only DNM2 was found to co-localise with the developing acrosomal vesicle. The specificity of antibody labelling was confirmed through the inclusion of negative controls (Neg) in which antibody buffer was substituted for the primary antibody. These experiments were replicated on material from three human donors and representative immunofluorescence images are shown. Insets are of equivalent sections shown at higher magnification.

**FIGURE 3. Immunofluorescence detection of dynamin isoforms within human spermatozoa.** Antibodies against (**A**) DNM1, (**B**) DNM2, and (**C**) DNM3 were used to determine the localisation of these proteins (red), in mature human spermatozoa. The acrosomal domain of these cells was subsequently counterstained with PNA. Higher magnification images of the dominant labelling patterns for each antibody are depicted on the right of panels (**A**), (**B**), and (**C**), Neg, Negative control (secondary antibody only). (**D - I**) The distinct labelling patterns for each dynamin isoform were quantified, with 100 cells being examined per sample. These studies were replicated with spermatozoa isolated from three different ejaculates of the same donor (**D**, **F**, and **H**) or single ejaculates from each of six different donors (**E**, **G**, and **I**).

**FIGURE 4. Examination of the effect of dynamin inhibition on the ability of human spermatozoa to engage in acrosomal exocytosis.** PNA staining was applied to record the acrosomal status of viable spermatozoa from each of several treatment groups. Cells were induced

to acrosome react via either a (**A**) progesterone (15 µM) or (Ubersax *et al.*) calcium ionophore (A23187, 2.5 µM) stimulus. (**A**) A significant reduction in the number of acrosome reacted cells was observed in the presence of dynamin inhibitors (Dynasore or Dyngo, 10 µM) when compared to treatment with either the vehicle control (DMSO) or an inactive isoform control (Dyngo-Ɵ). (Ubersax *et al.*) No such reduction was detected when acrosomal exocytosis was induced via A23187 challenge. Five biological replicates were conducted for each experiment and the results are presented as the means ± S.E.M. ***, $P < 0.001$; ****, $P < 0.0001$ compared to vehicle control (DMSO).

**FIGURE 5. Comparison of dynamin expression in the populations of good and poor quality human spermatozoa.** Two sub-populations comprising good and poor quality spermatozoa were generated via Percoll density gradient centrifugation of the same donor semen. (**A** and **B**) Immunolabelling of DNM1 revealed an equivalent staining pattern in both good and poor quality sub-populations of mature spermatozoa. (**C** and **D**) By contrast, immunolabelling of DNM2 demonstrated an apparent reduction in the amount of this protein in the head of poor quality spermatozoa (arrows) versus that of the good quality sub-population of cells. Spermatozoa from each of the two sub-populations were induced to acrosome react with either (**E**) progesterone (15 µM) or (**F**) calcium ionophore (A23187, 2.5 µM) stimulus. (**E** and **F**) The poor quality spermatozoa were significantly compromised ($P < 0.0001$) in their capacity to complete a progesterone, but not an A23187, induced acrosomal reaction compared to good quality spermatozoa. Non-Cap: the spermatozoa in these samples were not capacitated prior to the addition of progesterone or A23187. Cap: the spermatozoa in these samples were capacitated yet received no additional progesterone or A23187 stimulus. Five biological replicates were conducted with quantification of dynamin labelling and acrosomal status being performed across 100 cells per sample. Results are presented as the means ± S.E.M. ****, $P < 0.0001$.

**FIGURE 6. Immunofluorescence detection of cyclin dependent kinases (CDK1 and CDK5) in human spermatozoa.** (**A**) Immunolabelling of human spermatozoa with anti-CDK1 antibodies

revealed the strong labelling of the protein within the acrosomal and mid-piece domains. (**B**) Equivalent immunolabelling with anti-CDK5 antibodies demonstrated a restricted pattern of localisation within the mid-piece of the flagellum and no accompanying head labelling. (**A** and **B**) The specificity of antibody labelling was confirmed through the inclusion of negative controls (Neg) in which antibody buffer was substituted for the primary antibody. Three biological replicates were conducted and representative images are shown.

**FIGURE 7. Analysis of CDK1/dynamin 1 and CDK1/dynamin 2 interaction in human spermatozoa.** Proximity ligation assays (PLA) were applied to investigate the putative interaction between CDK1/DNM1 and CDK1/DNM2 in the anterior region of the human sperm head. This assay generates punctate red fluorescent signals when the targeted pair of proteins reside within a maximum of 40 nm from each other. A threshold of $\geqslant$3 red fluorescent spots within the sperm head was set for recording of positive PLA labelling. For clarity, cells were counterstained with the nuclear stain, DAPI. (**A**) Representative PLA images demonstrating that CDK1 resides in close proximity to DNM2, but not DNM1, in the anterior region of the sperm head. (**B**) The specificity of this interaction was confirmed through the use of antibodies targeting IZUMO1, a protein that is not expected to be a substrate of CDK1. (**C**) Data from this assay were quantified by recording the percentage of PLA positive spermatozoa, with 100 cells being examined per sample. Experiments were conducted on five biological replicates and the results are presented as the means ± S.E.M. *, $P < 0.05$ compared to progesterone treatment (CDK1/DNM2).

**FIGURE 8. Pharmacological inhibition of CDK1 reduces dynamin phosphorylation and the ability of human spermatozoa to acrosome react.** (**A**) Immunoblotting of lysates prepared from human spermatozoa incubated with CDK1 inhibitor (10 μM) revealed a reduction in the progesterone stimulated phosphorylation of DNM1-778/DNM2-764 residues compared to that cells treated with the vehicle alone (DMSO). Blots were stripped and re-probed with anti-DNM2 antibody to confirm equivalent levels of DNM2 in each sample. (**B**) The intensity of DNM1-

778/DNM2-764 labelling was quantified by Image J and normalized to DNM2 levels. (**C**) Immunofluorescent labelling of spermatozoa confirmed that the reduction in DNM1-778/DNM2-764 phosphorylation was restricted to the anterior (acrosomal) region of the sperm head (coinciding with the location of CDK1). (**D**) CDK1 inhibition also led to a significant reduction ($P < 0.01$) in the number of acrosome reacted cells following treatment with progesterone when compared to the vehicle only control (DMSO). All experiments were conducted on five biological replicates and the results are presented as the means ± S.E.M. ***, $P < 0.001$; ****, $P < 0.0001$ compared to DMSO vehicle control.

**SUPPLEMENTARY FIGURE S1. Examination of the specificity of anti-dynamin 2 antibody localisation patterns.** Representative immunofluorescence images indicate that DNM2 is (**A**) localised to the developing sperm acrosome in testicular tissue (arrowheads), and to the (**B**) corresponding anterior region of the mature sperm head (arrowheads). (**A** and **B**) Both of these localisation patterns were abolished following pre-absorption of the antibody with excess immunizing peptide (+IP). (**B**) In contrast, an additional focus of mid-piece labelling that was detected in mature spermatozoa persisted despite the pre-absorption of the anti-DNM2 antibody with immunizing peptide, suggesting that this is non-specific. (**A**) DAPI and (**A** and **B**) PNA were used to counterstain cells to and detect nuclei (blue) and acrosome, respectively. For clarity, the peripheral structure of seminiferous tubules are outlined with dotted lines.

**SUPPLEMENTARY FIGURE S2. Detection of dynamin 1 in the human epididymis.** (**A**) The localisation of DNM1 (arrows) was examined in human epididymal sections by sequential labelling with anti-DNM1 antibody and propidium iodide (PI, red). Epithelial cells lining the epididymal duct and spermatozoa within the epididymal lumen were both found to display DNM1 labelling. Representative negative control (Neg, secondary antibody only) images are included to demonstrate the specificity of antibody labelling. ep, epithelial cells; sp, sperm; int, interstitium; l, lumen. (**B**)

Immunoblotting was also employed to detection the presence of DNM1 in whole seminal fluid as well as an extracellular vesicle fraction isolated from seminal fluid via Optiprep density gradient centrifugation.

**SUPPLEMENTARY FIGURE S3. Immunogold labelling of dynamin 2 in head of human spermatozoa.** Electron microscopy was used in conjunction with immunogold secondary antibody to investigate the ultrastructural localisation of DNM2 in the acrosomal domain of human spermatozoa. No equivalent labelling was observed in the negative control samples (Neg) probed with secondary antibody only.

**SUPPLEMENTARY FIGURE S4. Optimisation of a robust, progesterone-induced acrosome reaction assay via manipulation of the pH (6.4 - 7.8) of the BWW incubation medium.** (A) Acrosome reaction rates were found to be consistently elevated in BWW with an adjusted pH of 7.00 - 7.05; thus, these condition were applied for all subsequent acrosome reaction assays. (**B**) Representative images illustrative of the PNA labelling criteria used to determine acrosome status; a complete absence PNA labelling, or restriction of PNA labelling to the equatorial domain, was used define acrosome reacted sperm cells (arrowheads in contrast with arrows). Three biological replicates were conducted.

**SUPPLEMENTARY FIGURE S5. Effect of pharmacological inhibitors on sperm motility.** (**A** and **B**) Of all the pharmacological inhibitors used in this study, only Dyngo 4a (10 µM) was found to have a significant negative impact on human sperm motility ($P < 0.05$) compared to DMSO vehicle control. Importantly, this reduction in motility was not accompanied by an equivalent reduction in cell vitality, which remained above 75% in all treatment groups. Five biological replicates were conducted and quantification of results are presented as the means ± S.E.M. *, $P < 0.05$.

**SUPPLEMENTARY FIGURE S6. Analysis of CDK1/dynamin 1 and CDK1/dynamin 2 interaction in human spermatozoa**. PLA was applied to investigate the putative interaction

between CDK1/DNM1 and CDK1/DNM2 in the anterior region of the human sperm head. Data presented are representative cell population images (positive cells indicated by arrows) corresponding to the individual cells presented in Figure 7.

**SUPPLEMENTARY FIGURE S7. Confirmation that anti-DNM1-Ser778 antibody also recognises phosphorylated DNM2-Ser764.** An immunoprecipitation strategy with anti-DNM2 antibody was used to pull-down DNM2 from sperm lysates. Captured protein were eluted from protein G beads and immunoblotting was used to detect DNM2 and DNM2-Ser764 by anti DNM2 and DNM1-Ser778 antibodies. Alongside with elution are antibody-only control (Ab control), bead-only control (Bead control), progesterone treated sperm lysate (Input) and precleared control (Preclear); Mouse brain lysate was used as positive control to indicate the location of the band.

**SUPPLEMENTARY FIGURE S8. Colocalisation of CDK1 and phospho-DNM1-778/DNM2-764 in capacitated populations of human spermatozoa treated with progesterone.** Representative immunofluorescence images depicting spermatozoa positively labelled with anti-CDK1 (red) and anti-phospho-DNM1-778/DNM2-764 antibodies. Co-localisation of the target antigens was detected in the anterior region of the sperm head (arrows) and the neck/mid-piece of the flagellum.

**SUPPLEMENTARY FIGURE S9. Colocalisation of phospho-DNM1-778/DNM2-764 and PNA in capacitated populations of human spermatozoa treated with progesterone.** Representative immunofluorescence images depicting spermatozoa positively labelled with PNA in the acrosomal region. These acrosome intact cells were also positively labelled with anti-DNM1-778/DNM2-764 antibodies (arrow). In contrast, the loss of acrosomal contents (denoted by an absence of PNA labelling, arrow heads) was accompanied by a reduction/loss of anti-DNM1-778/DNM2-764 antibody labelling within this domain. Negative control: secondary antibody only.

Figure 1

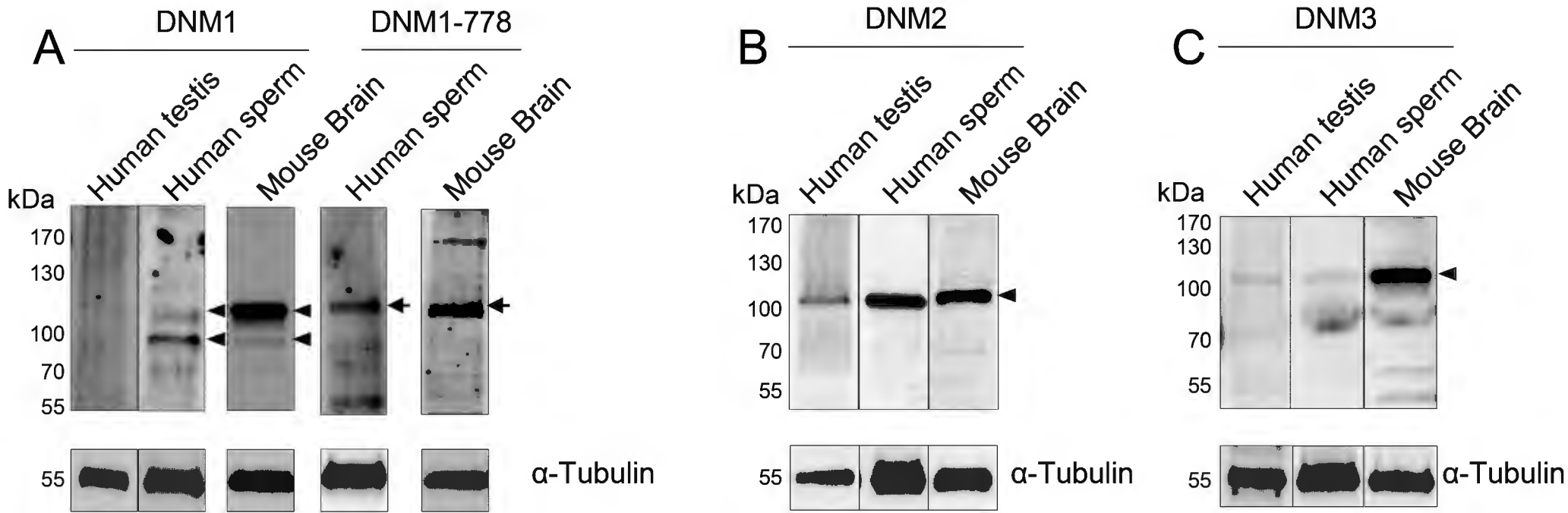
A
DNM1
DNM1-778
Human testis
Human sperm
Mouse Brain
Human sperm
Mouse Brain
kDa
170
130
100
70
55
55
α-Tubulin
B
DNM2
Human testis
Human sperm
Mouse Brain
kDa
170
130
100
70
55
55
α-Tubulin
C
DNM3
Human testis
Human sperm
Mouse Brain
kDa
170
130
100
70
55
55
α-Tubulin

Figure 2

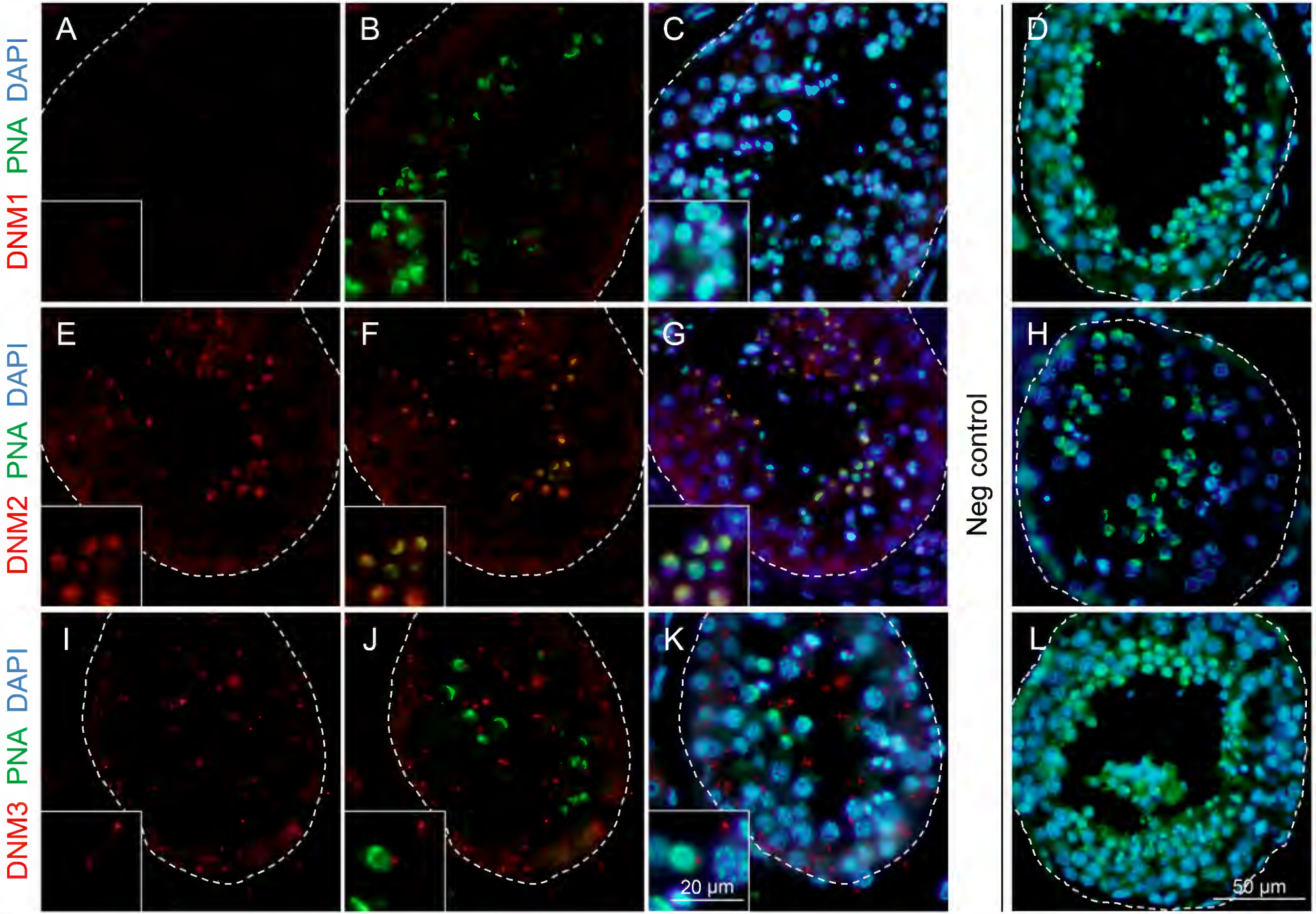
A
B
C
D
E
F
G
H
I
J
K
L
DNM1 PNA DAPI
DNM2 PNA DAPI
DNM3 PNA DAPI
Neg control
20 µm
50 µm

Figure 3

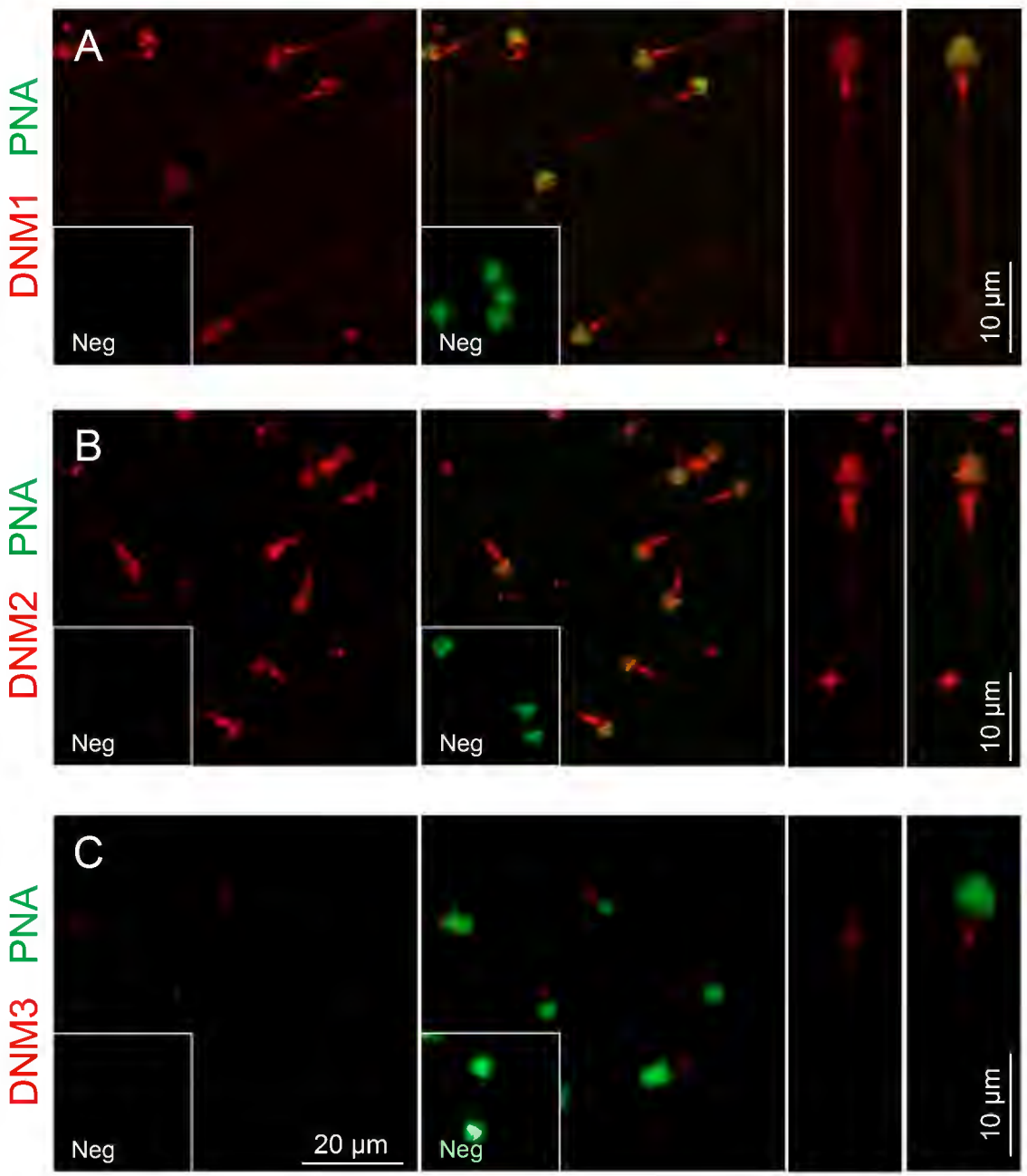
A
DNM1 PNA
Neg
Neg
10 µm
B
DNM2 PNA
Neg
Neg
10 µm
C
DNM3 PNA
Neg
20 µm
Neg
10 µm

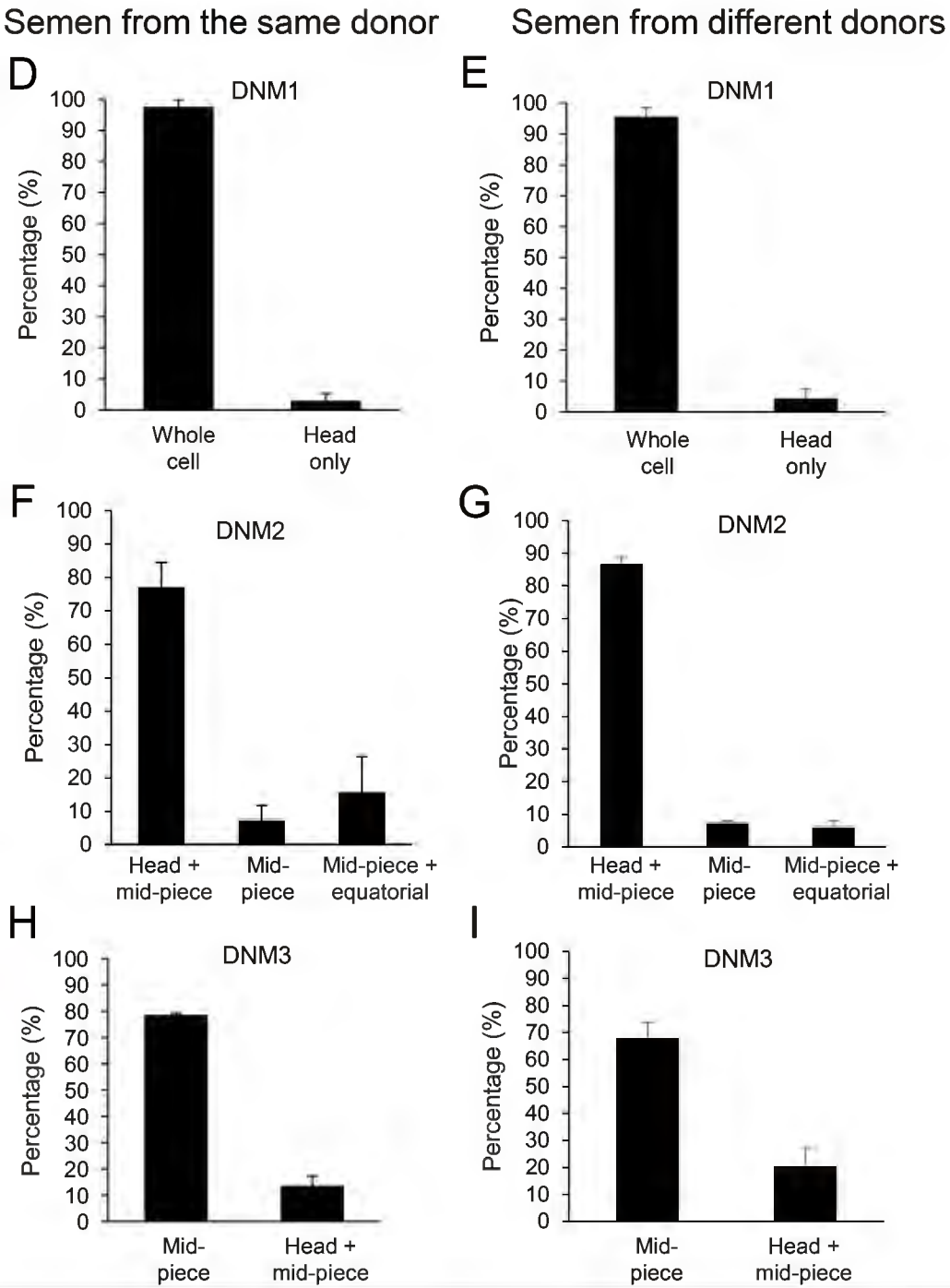
Semen from the same donor
Semen from different donors
D
DNM1
Percentage (%)
Whole cell
Head only
E
DNM1
Percentage (%)
Whole cell
Head only
F
DNM2
Percentage (%)
Head + mid-piece
Mid-piece
Mid-piece + equatorial
G
DNM2
Percentage (%)
Head + mid-piece
Mid-piece
Mid-piece + equatorial
H
DNM3
Percentage (%)
Mid-piece
Head + mid-piece
I
DNM3
Percentage (%)
Mid-piece
Head + mid-piece

Figure 4

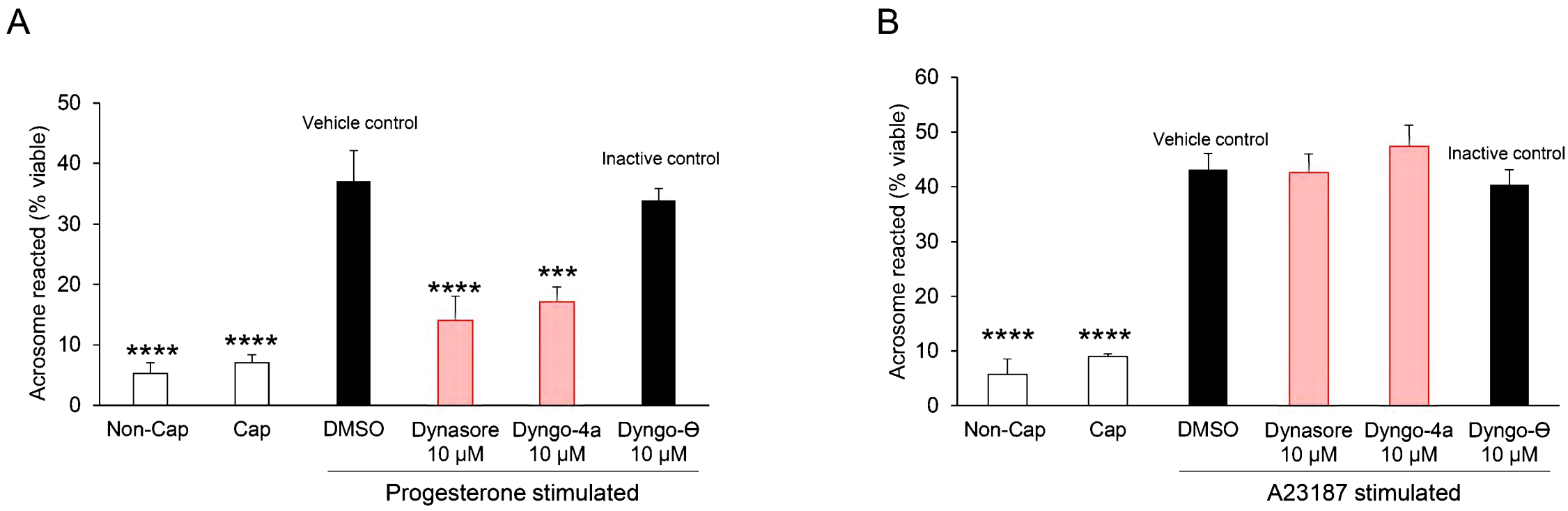
A
Acrosome reacted (% viable)
50
40
30
20
10
0
Vehicle control
Inactive control
****
****
****
***
Non-Cap
Cap
DMSO
Dynasore 10 μM
Dyngo-4a 10 μM
Dyngo-Θ 10 μM
Progesterone stimulated
B
Acrosome reacted (% viable)
60
50
40
30
20
10
0
Vehicle control
Inactive control
****
****
Non-Cap
Cap
DMSO
Dynasore 10 μM
Dyngo-4a 10 μM
Dyngo-Θ 10 μM
A23187 stimulated

Figure 5

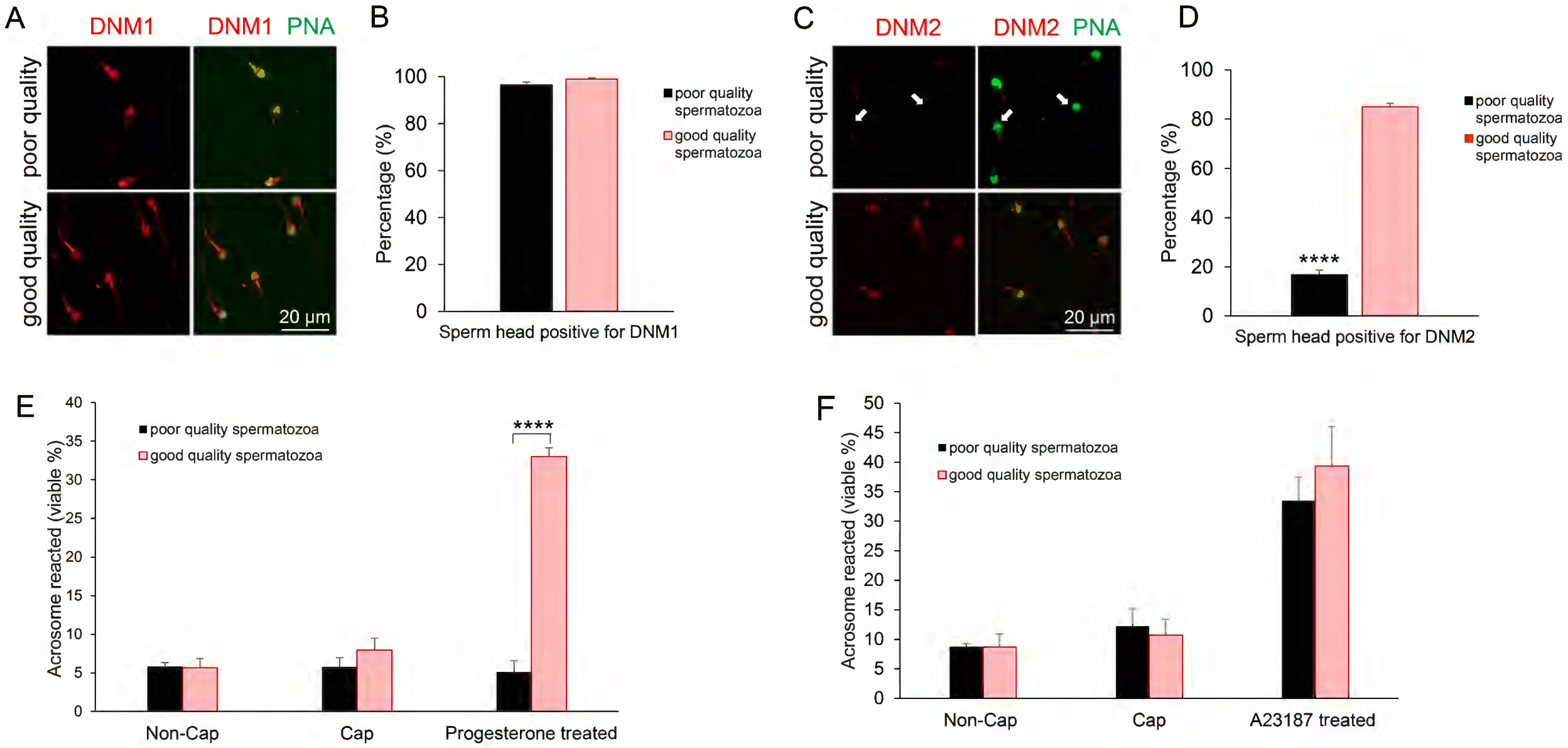
A
DNM1
DNM1 PNA
poor quality
good quality
20 µm
B
Percentage (%)
100
80
60
40
20
0
poor quality spermatozoa
good quality spermatozoa
Sperm head positive for DNM1
C
DNM2
DNM2 PNA
poor quality
good quality
20 µm
D
Percentage (%)
****
Sperm head positive for DNM2
E
Acrosome reacted (viable %)
poor quality spermatozoa
good quality spermatozoa
****
Non-Cap
Cap
Progesterone treated
F
Acrosome reacted (viable %)
poor quality spermatozoa
good quality spermatozoa
Non-Cap
Cap
A23187 treated

Figure 6

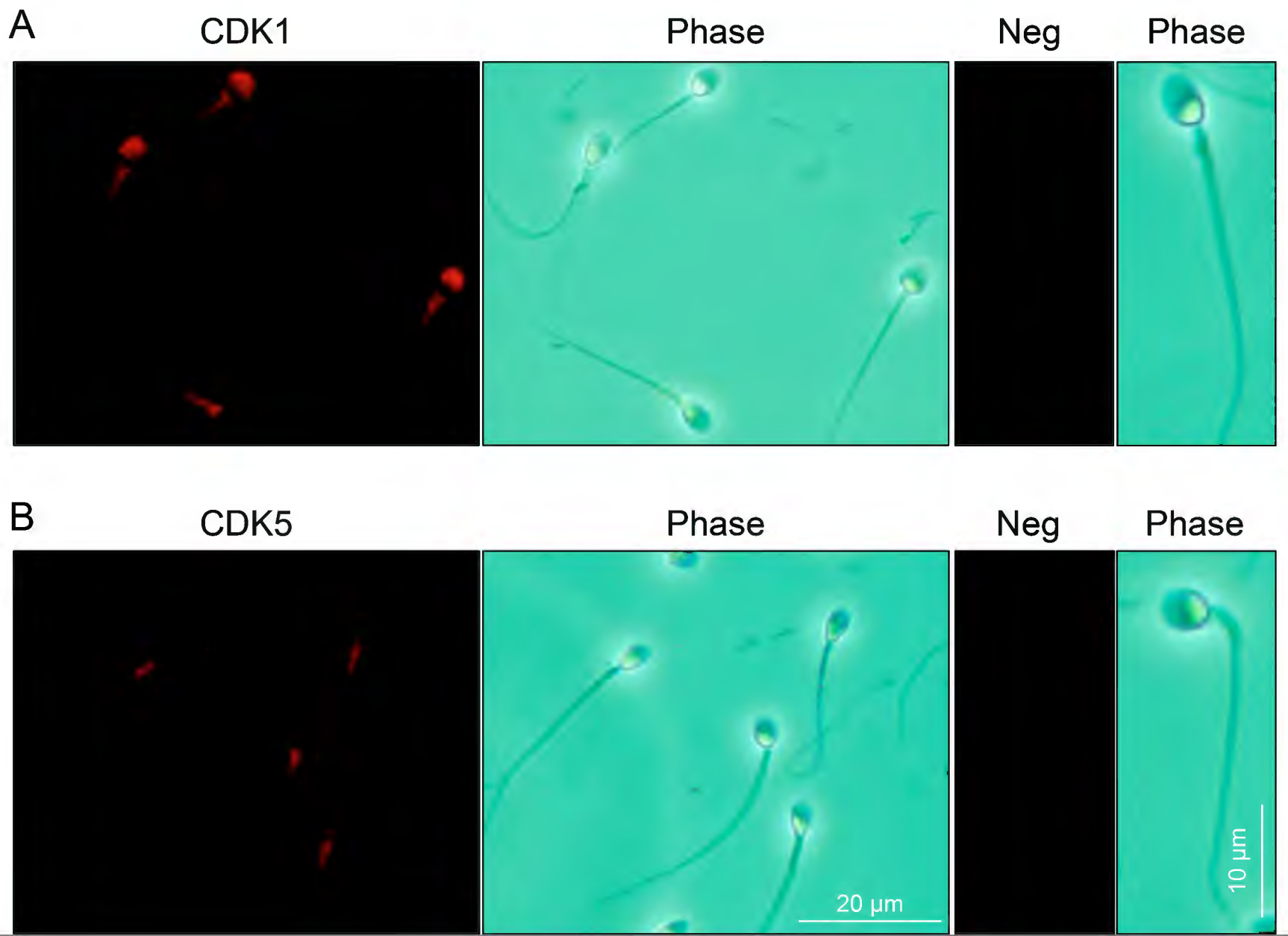

Figure 7

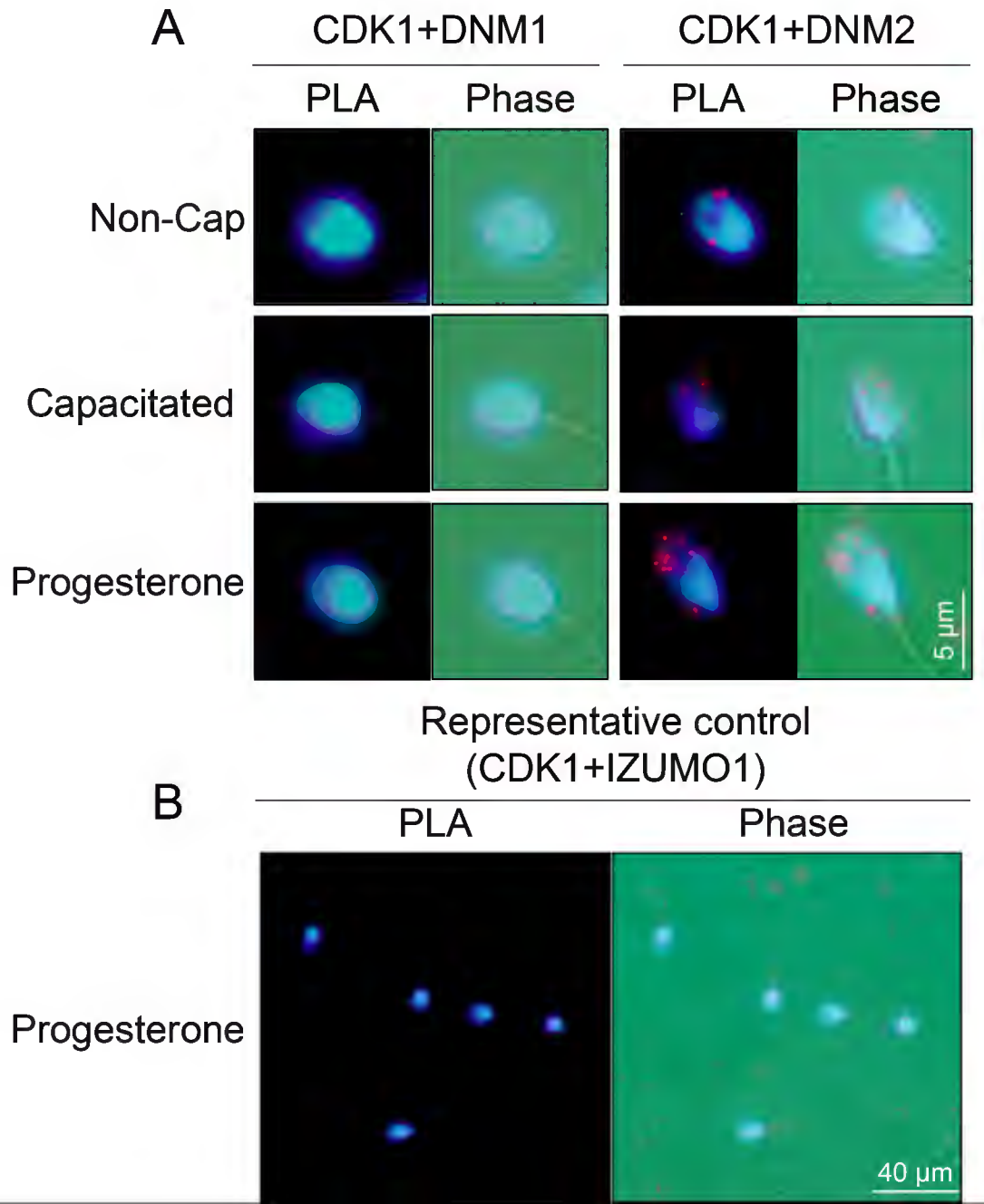
A
CDK1+DNM1
CDK1+DNM2
PLA
Phase
PLA
Phase
Non-Cap
Capacitated
Progesterone
5 µm
B
Representative control
(CDK1+IZUMO1)
PLA
Phase
Progesterone
40 µm

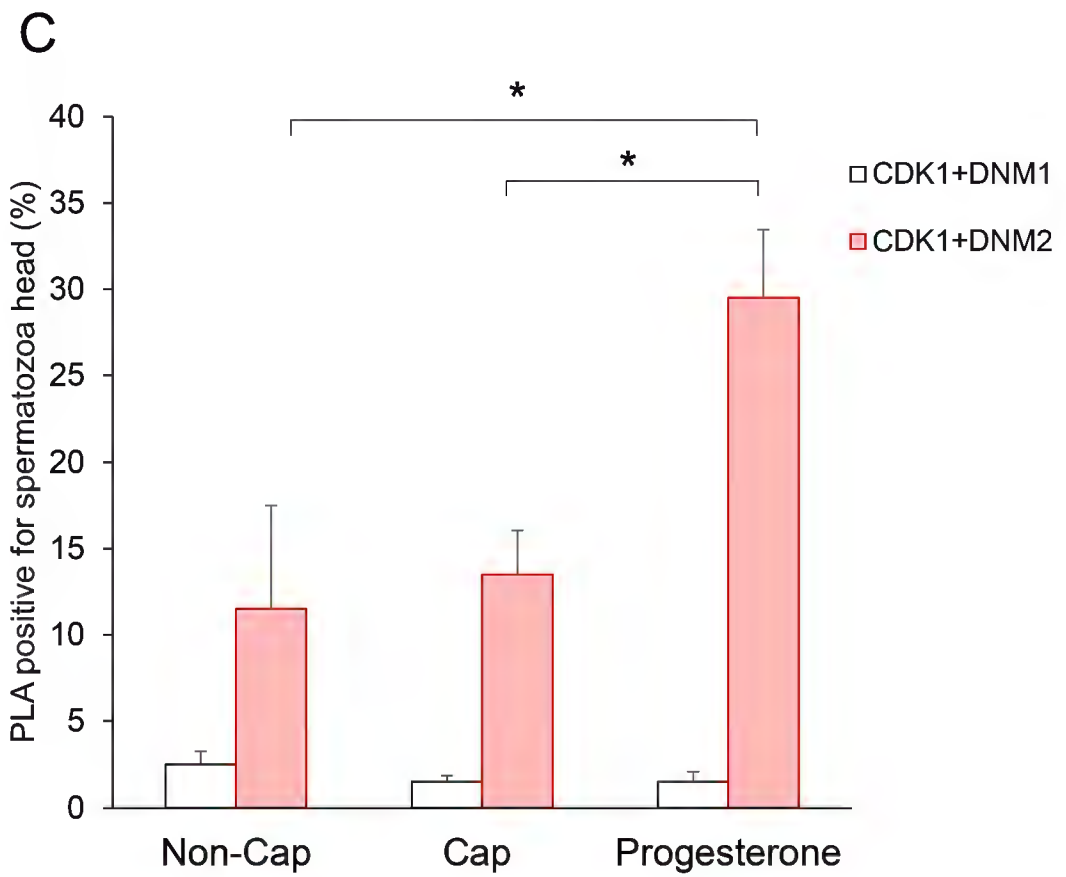
C
PLA positive for spermatozoa head (%)
0
5
10
15
20
25
30
35
40
*
*
Non-Cap
Cap
Progesterone
CDK1+DNM1
CDK1+DNM2

Figure 8

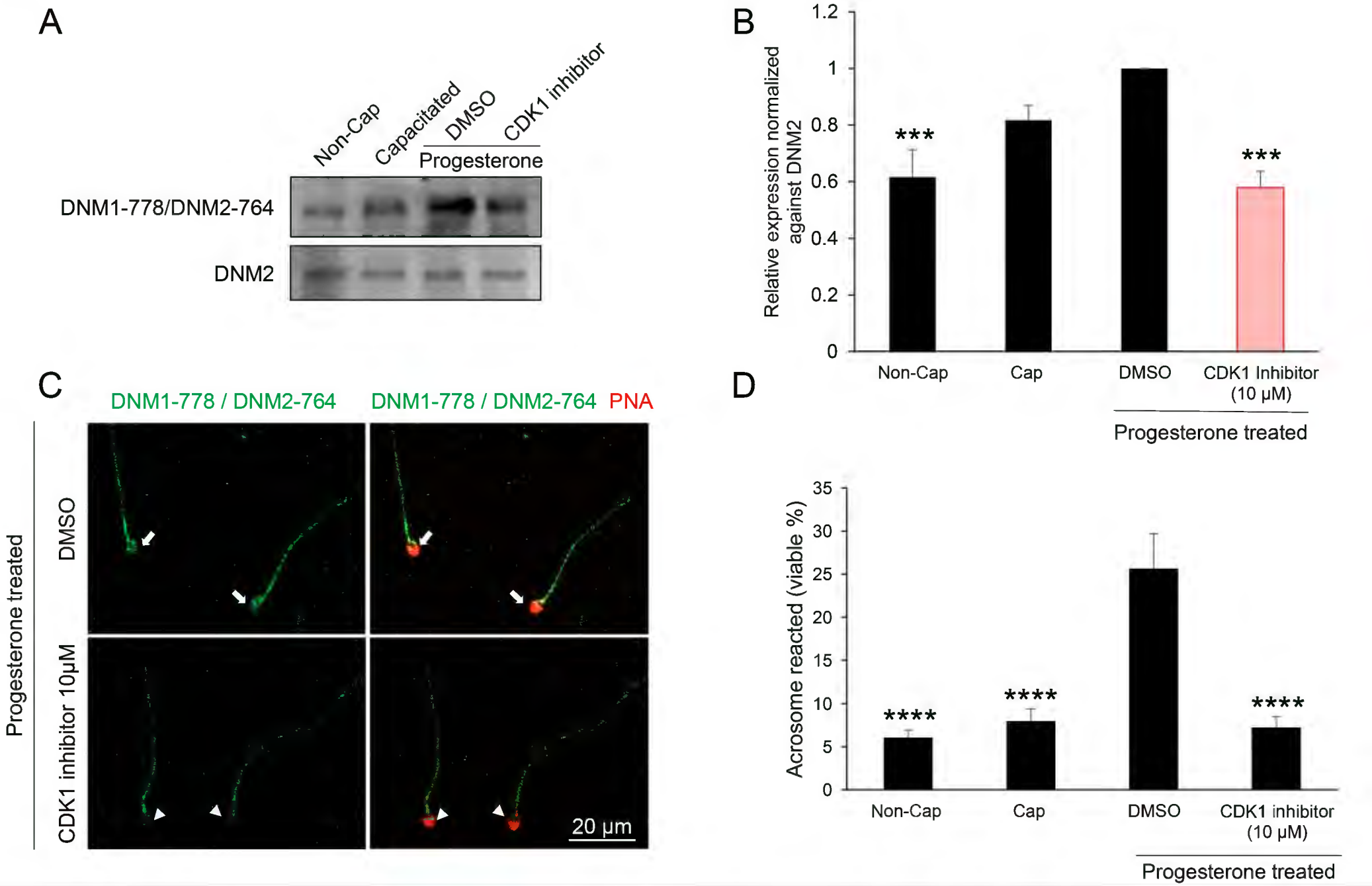
A
Non-Cap
Capacitated
DMSO
CDK1 inhibitor
Progesterone
DNM1-778/DNM2-764
DNM2
B
Relative expression normalized against DNM2
1.2
1
0.8
0.6
0.4
0.2
0
***
***
Non-Cap
Cap
DMSO
CDK1 Inhibitor (10 μM)
Progesterone treated
C
DNM1-778 / DNM2-764
DNM1-778 / DNM2-764 PNA
Progesterone treated
DMSO
CDK1 inhibitor 10μM
20 μm
D
Acrosome reacted (viable %)
35
30
25
20
15
10
5
0
****
****
****
Non-Cap
Cap
DMSO
CDK1 inhibitor (10 μM)
Progesterone treated